Investigation and Development of Zwitterionic Biomaterials for Protein Therapeutics

Sijun Liu

A dissertation

submitted in partial fulfillment of the

requirements for the degree of

Doctor of Philosophy

University of Washington

2016

Reading Committee:

Shaoyi Jiang, Chair

Suzie H. Pun

Ying Zheng

Program Authorized to Offer Degree:

Department of Bioengineering

© Copyright 2016

Sijun Liu

University of Washington

Abstract

Investigation and Development of Zwitterionic Biomaterials

for Protein Therapeutics

Sijun Liu

Chair of the Supervisory Committee:
Professor Shaoyi Jiang
Chemical Engineering

Proteins offer significant therapeutic potential over small-molecule drugs for many disease treatments, but they are more fragile and sensitive to environmental stress. The synthetic polymer poly(ethylene glycol) (PEG) has been used to increase protein size for prolonged circulation as well as act as a steric shield of immunogenic epitopes. However, it may interfere with substrate binding at the active site or elicit antibody responses toward itself, highlighting a need for an alternative strategy. This dissertation is a compilation of such efforts, specifically the development of zwitterionic materials for protein delivery. The champion zwitterionic polymer poly(carboxybetaine) (PCB) is a superhydrophilic macromolecule that is biomimetic, based on the naturally occurring amino-acid derivative trimethylglycine. **We hypothesize that a polyzwitterion-protein conjugate will exhibit enhanced circulation without sacrificing enzyme activity or eliciting undesirable immune responses.** This is tested in the context of immunogenic proteins and proteins with poor circulation residence times and examined in the following chapters: (1) introduction of zwitterionic materials, (2) synthesis of biocompatible zwitterionic polymers for bioconjugation, (3) direct comparison between same solution-size PEG and PCB in protecting an immunogenic therapeutic enzyme, (4) effect of varying polymer size and conjugation density on protein protection, and (5) preclinical investigations of a novel polymer-protein conjugate.

To my dear mother

&

To whom I owe everything

ACKNOWLEDGMENTS

First and foremost, I must thank my thesis advisor, Dr. Shaoyi Jiang, for his patience, support, and motivation during the last five years. I sincerely appreciate the insightful comments and critiques from Dr. Jiang and the rest of my supervisory committee: Drs. Dayong Gao, Suzie Pun, Kim Woodrow, and Ying Zheng. Together, their extensive combined technical expertise greatly assisted me in shaping my experimental planning and research training. In addition, past and present members of the Jiang research group were instrumental in mentoring and helping me accomplish my research goals. I could not ask for a better support system during my PhD career.

I would also like to recognize the following colleagues and comrades in no particular order:

- Dr. Alexander J. Mastroianni, who inspired me to pursue graduate studies and exemplifies the kind of researcher I aspire to be: patient, inquisitive, kind, and generous.
- Dr. James-Kevin Y. Tan, whose friendship and companionship I cherish ever since the dreary days of interview weekend. Thank you for sharing your sartorial expertise and joining me in countless bubble milk tea excursions near and far.
- Mr. John K. Katahara, for listening, eating our feelings together, and always making me laugh when I need it. Thank you for four years of baked goods and explorations.
- My lunch crew, which I fondly nicknamed “the ChemE kids,” for welcoming this Bioengineering expatriate into their fold. Thank you for all the caffeine therapy and sincere/silly/scandalous conversations, Mr. Kyle B. Caldwell, Mr. Matthew J. Crane, Ms. Elisa T. Harrison, Mr. Edward L. Michor, Ms. Elena P. Pandres, and Mr. William E. Voje, Jr.
- Dr. David S. H. Chu, for being the older brother I always wanted, making fried chicken and apple cider runs, and trash-talking rival football fans for me.
- Dr. Kari Thorkelsson, for being a reliable chocolate supplier and dedicated book reviewer.

Finally, I reserve the utmost gratitude for my family, who gave me endless unconditional support and indulged my refusal to grow up and get a real job. A special thanks to the women in my life, for teaching me by example loyalty, optimism, and above all, perseverance.

Thank you everyone, from the bottom of my heart.

TABLE OF CONTENTS

LIST OF FIGURES

LIST OF SCHEMES

LIST OF TABLES

CHAPTER 1

INTRODUCTION

1.1 Nonfouling zwitterionic materials

Zwitterion derives the first part of its name from the German word for "hybrid," which describes the equimolar presence of positively and negatively charged groups in an overall neutrally charged molecule. A notable example is betaines, which are zwitterions in which the positive charge is a quaternary ion with no hydrogen (**Scheme 1-1**). These molecules have interesting properties, such as their ability to resist protein adsorption (so-called nonfouling properties) when attached to a surface. Early work suggested that this phenomenon correlates with the high charge density of its anion and low charge density of its cation.[1,2] This particular combination of ion pairs is described by the Hofmeister series[3] (**Figure 1-1**) to cause water to favorably interact and promote intramolecular interactions in proteins, but no explanation was given as to why this occurs. More recently, a rigorous study into the mechanisms of nonfouling zwitterions demonstrated that it is intrinsically nonfouling: when a surface does not have a 1:1 ratio of cations and anions, it loses the ability to resist protein adsorption.[4] This balance in charge minimizes the dipole moments on the surface, allowing zwitterions to form a hydration layer through electrostatic interactions and is fundamentally different from neutral hydrophilic polymers, which binds water through hydrogen bonding. These attractive properties prompted significant research into transforming these ions into polymeric materials with ultra-low fouling characteristics.

Fouling resistance is highly desirable in biomedical applications. When nanomaterials enter the blood stream, they are immediately inundated with serum proteins that may adsorb and doom them to failure: these opsonins can cover trafficking capabilities, prevent intended receptor binding, and mark the material for phagocytosis and rapid clearance, among many other effects. [5,6] Similarly, detection of specific analytes in blood is difficult due to adsorption of these serum proteins onto the sensor surface. Recent efforts in polyzwitterionic materials have exploited their nonfouling properties to combat these challenges. Notably, polyzwitterionic surfaces have <5 ng/cm^2 protein adsorbed in single-protein

solutions as well as undiluted blood plasma and serum.[7] Zwitterion-functionalized sensors can detect glucose in blood with high accuracy[8] long after the commercial sensor has failed, as well as measuring fructose concentration in complex media[9] via surface-enhanced Raman spectroscopy methods. Implants shielded under a zwitterion hydrogel resisted the foreign body response of capsule formation for the full study time of three months.[10] Zwitterion-based nanoparticles exhibit remarkable circulation times in small animal models.[11-13] More recently, the arsenal of zwitterionic materials have expanded to hydrogels for preservation of stem cells from differentiation[14] and applications of natural zwitterions[15,16] like nonfouling peptides. The specific application of protein conjugation by polyzwitterions will be discussed in full detail in the rest of the dissertation.

1.2 The main competition: advantages and drawbacks

1.2.1 The nonionic polymer poly(ethylene glycol)

Poly(ethylene glycol), also known as poly(ethylene oxide) or PEG, is the reigning standard of neutral synthetic polymers for biological applications. It is synthesized via ring-opening polymerization of ethylene oxide, and can achieve polymers with narrow size distributions (low polydispersity).[17] Often referenced as a hydrophilic polymer, PEG is in actuality amphiphilic: its ether groups are hydrogen-bond acceptors, but the ethylene backbone is hydrophobic. This allows PEG to dissolve in various organic solvents such as dichloromethane, acetone, and toluene in addition to water. PEG is uniquely amphiphilic in that similar polymers, such as poly(methylene oxide) and poly(propylene oxide), are completely insoluble in water (**Scheme 1-2**).[18] Due to these precisely located ether groups, PEG can bind large quantities of water molecules via aforementioned hydrogen bonding, allowing it to adopt a balloon-like conformation and exclude materials from its vicinity. This manifests as an ability to prevent protein adsorption, giving PEG nonfouling capabilities much like polyzwitterions.

This water binding ability is why PEG is the preferred polymer for protein modification. Its conjugation increases the overall size of the biomacromolecule while providing a steric shell. This prevents nonspecific binding of serum proteins and shields immunogenic epitopes from recognition. However, despite this protection, PEG attachment (PEGylation) often requires a compromise in bioactivity. As the catalytic or active site of an enzyme is often hydrophobic, it can adversely interact

with PEG and block proper binding of substrates.[19-21] This is trivial when the substrate is small and can diffuse through the polymer mesh, but becomes a significant hurdle when the substrate is a macromolecule like peptides or other proteins.

1.2.2 Immunogenicity towards PEG

Further complicating the benefits of PEG is its apparent hapten-like properties. A hapten is a molecule that does not exhibit immunogenic properties until it is attached to a larger carrier. Unfortunately, this is precisely the scenario of PEGylation. While it has been classified as "generally recognized as safe (GRAS)" by the Food and Drug Administration, recent reports in the scientific and medical communities have highlighted the emergence of antibody responses. PEG-specific antibodies have been observed in healthy blood donors[22-24], patients receiving PEGylated proteins[23,25,26], and laboratory animals exposed to PEGylated nanomaterials[12,26-29].

PEG-specific antibodies were reported as early as 1983, in which animals were immunized against PEG and PEGylated immunogenic proteins[30]. The researchers concluded that PEG becomes immunogenic as a function of the immunogenicity of the carrier protein as well as the density of grafted polymers. With decreasing polymer attachment (i.e. lower surface coverage) or increasingly foreign protein (i.e. more recognizable epitopes), the anti-PEG antibody response becomes more robust. Furthermore, evidence suggests that the hydrophobicity of amphiphilic PEG contributes to possible immune responses against it: the antibody decreases when the end group changes from *t*-butoxycarbonyl to methoxy to hydroxyl[31]. Follow-up work also demonstrated that two types of anti-PEG antibodies were generated, one towards the backbone of PEG and one that is more specific for the end group, and these antibodies may recognize as few as three repeat units[32].

The consequence of such antibodies may be rapid blood clearance of PEGylated therapeutics, causing loss in efficacy or resistance to treatment. These drawbacks are major flaws and are the motivation for adapting zwitterionic materials as an alternative platform, the goals of this thesis.

1.3 Figures and schemes

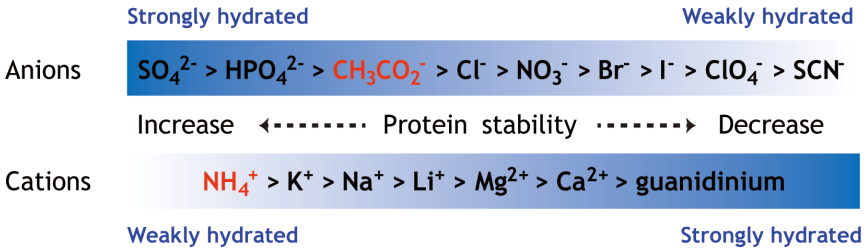

Figure 1-1: The Hofmeister series describing ion interactions with proteins. A strongly hydrated anion and weakly hydrated cation pair stabilizes proteins, while the opposite destabilizes them. In red are the ion pairs present in glycine betaine and carboxybetaine.

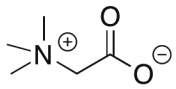

Glycine betaine

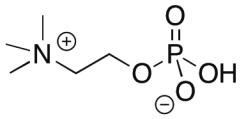

Phosphocholine

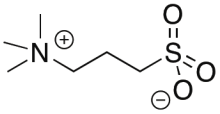

Sulfobetaine

Scheme 1-1: Chemical structures of common zwitterions.

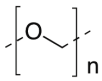

Poly(methylene oxide)

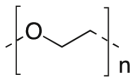

Poly(ethylene glycol)

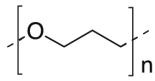

Poly(propylene oxide)

Scheme 1-2: Chemical structures of PEG and PEG-like polymers

1.4 References

1 Kane, R. S., Deschatelets, P. & Whitesides, G. M. Kosmotropes form the basis of protein-resistant surfaces. *Langmuir* **19**, 2388-2391, doi:10.1021/la020737x (2003).

2 Zhang, Y. J. & Cremer, P. S. Interactions between macromolecules and ions: the Hofmeister series. *Current Opinion in Chemical Biology* **10**, 658-663, doi:10.1016/j.cbpa.2006.09.020 (2006).

3 Kunz, W., Henle, J. & Ninham, B. W. 'Zur Lehre von der Wirkung der Salze' (about the science of the effect of salts): Franz Hofmeister's historical papers. *Current Opinion in Colloid & Interface Science* **9**, 19-37, doi:10.1016/j.cocis.2004.05.005 (2004).

4 Chen, S. F., Zheng, J., Li, L. Y. & Jiang, S. Y. Strong resistance of phosphorylcholine self-assembled monolayers to protein adsorption: Insights into nonfouling properties of zwitterionic materials. *Journal of the American Chemical Society* **127**, 14473-14478, doi:10.1021/ja054169u (2005).

5 Salvati, A., Pitek, A. S., Monopoli, M. P., Prapainop, K., Bombelli, F. B. *et al*. Transferrin-functionalized nanoparticles lose their targeting capabilities when a biomolecule corona adsorbs on the surface. *Nature Nanotechnology* **8**, 137-143, doi:10.1038/nnano.2012.237 (2013).

6 Lesniak, A., Fenaroli, F., Monopoli, M. R., Aberg, C., Dawson, K. A. *et al*. Effects of the Presence or Absence of a Protein Corona on Silica Nanoparticle Uptake and Impact on Cells. *Acs Nano* **6**, 5845-5857, doi:10.1021/nn300223w (2012).

7 Ladd, J., Zhang, Z., Chen, S., Hower, J. C. & Jiang, S. Zwitterionic polymers exhibiting high resistance to nonspecific protein adsorption from human serum and plasma. *Biomacromolecules* **9**, 1357-1361, doi:10.1021/bm701301s (2008).

8 Yang, W., Xue, H., Carr, L. R., Wang, J. & Jiang, S. Y. Zwitterionic poly(carboxybetaine) hydrogels for glucose biosensors in complex media. *Biosensors & Bioelectronics* **26**, 2454-2459, doi:10.1016/j.bios.2010.10.031 (2011).

9 Sun, F., Bai, T., Zhang, L., Ella-Menye, J.-R., Liu, S. *et al*. Sensitive and Fast Detection of Fructose in Complex Media via Symmetry Breaking and Signal Amplification Using Surface-Enhanced Raman Spectroscopy. *Analytical Chemistry* **86**, 2387-2394, doi:10.1021/ac4040983 (2014).

10 Zhang, L., Cao, Z. Q., Bai, T., Carr, L., Ella-Menye, J. R. *et al*. Zwitterionic hydrogels implanted in mice resist the foreign-body reaction. *Nature Biotechnology* **31**, 553-+, doi:10.1038/nbt.2580 (2013).

11 Cao, Z. Q., Zhang, L. & Jiang, S. Superhydrophilic Zwitterionic Polymers Stabilize Liposomes. *Langmuir* **28**, 11625-11632, doi:10.1021/la302433a (2012).

12 Yang, W., Liu, S., Bai, T., Keefe, A. J., Zhang, L. *et al*. Poly(carboxybetaine) nanomaterials enable long circulation and prevent polymer-specific antibody production. *Nano Today* **9**, 10-16, doi:10.1016/j.nantod.2014.02.004 (2014).

13 Zhang, L., Cao, Z. Q., Li, Y. T., Ella-Menye, J. R., Bai, T. *et al*. Softer Zwitterionic Nanogels for Longer Circulation and Lower Splenic Accumulation. *Acs Nano* **6**, 6681-6686, doi:10.1021/nn301159a (2012).

14 Bai, T., Sun, F., Zhang, L., Sinclair, A., Liu, S. *et al*. Restraint of the Differentiation of Mesenchymal Stem Cells by a Nonfouling Zwitterionic Hydrogel. *Angewandte Chemie-International Edition* **53**, 12729-12734, doi:10.1002/anie.201405930 (2014).

15 Liu, E. J., Sinclair, A., Keefe, A. J., Nannenga, B. L., Coyle, B. L. *et al*. EKylation: Addition of an Alternating-Charge Peptide Stabilizes Proteins. *Biomacromolecules* **16**, 3357-3361, doi:10.1021/acs.biomac.5b01031 (2015).

16 Nowinski, A. K., White, A. D., Keefe, A. J. & Jiang, S. Y. Biologically Inspired Stealth Peptide-Capped Gold Nanoparticles. *Langmuir* **30**, 1864-1870, doi:10.1021/la404980g (2014).

17 Harris, J. M. *Poly(ethylene glycol) Chemistry: Biotechnical and Biomedical Applications*. (Springer Science, 1992).

18 Bailey, F. E. & Koleske, J. V. *Alkylene oxides and Their Polymers*. (CRC Press, 1990).

19 Bailon, P., Palleroni, A., Schaffer, C. A., Spence, C. L., Fung, W. J. *et al*. Rational design of a potent, long-lasting form of interferon: A 40 kDa branched polyethylene glycol-conjugated

interferon alpha-2a for the treatment of hepatitis C. *Bioconjugate Chemistry* **12**, 195-202, doi:10.1021/bc000082g (2001).

20 Monkarsh, S. P., Ma, Y. M., Aglione, A., Bailon, P., Ciolek, D. *et al*. Positional isomers of monopegylated interferon alpha-2a: Isolation, characterization, and biological activity. *Analytical Biochemistry* **247**, 434-440, doi:10.1006/abio.1997.2128 (1997).

21 Pelegri-O'Day, E. M., Lin, E. W. & Maynard, H. D. Therapeutic Protein-Polymer Conjugates: Advancing Beyond PEGylation. *Journal of the American Chemical Society* **136**, 14323-14332, doi:10.1021/ja504390x (2014).

22 Richter, A. W. & Akerblom, E. Polyethylene-glycol reactive antibodies in man - titer distribution in allergic patients treated with monomethoxy polyethylene-glycol modified allergens or placebo, and in healthy blood-donors. *International Archives of Allergy and Applied Immunology* **74**, 36-39 (1984).

23 Garay, R. P., El-Gewely, R., Armstrong, J. K., Garratty, G. & Richette, P. Antibodies against polyethylene glycol in healthy subjects and in patients treated with PEG-conjugated agents. *Expert Opinion on Drug Delivery* **9**, 1319-1323, doi:10.1517/17425247.2012.720969 (2012).

24 Leger, R. M., Arndt, P., Garratty, G., Armstrong, J. K., Meiselman, H. J. *et al*. Normal donor sera can contain antibodies to polyethylene glycol (PEG). *Transfusion* **41**, 29S-30S (2001).

25 Armstrong, J. K., Hempel, G., Koling, S., Chan, L. S., Fisher, T. *et al*. Antibody against poly(ethylene glycol) adversely affects PEG-asparaginase therapy in acute lymphoblastic leukemia patients. *Cancer* **110**, 103-111, doi:10.1002/cncr.22739 (2007).

26 Hershfield, M. S., Roberts, L. J., II, Ganson, N. J., Kelly, S. J., Santisteban, I. *et al*. Treating gout with pegloticase, a PEGylated urate oxidase, provides insight into the importance of uric acid as an antioxidant in vivo. *Proceedings of the National Academy of Sciences of the United States of America* **107**, 14351-14356, doi:10.1073/pnas.1001072107 (2010).

27 Ishida, T., Kashima, S. & Kiwada, H. The contribution of phagocytic activity of liver macrophages to the accelerated blood clearance (ABC) phenomenon of PEGylated liposomes in rats. *Journal of Controlled Release* **126**, 162-165, doi:10.1016/j.jconrel.2007.11.009 (2008).

28 Shimizu, T., Ichihara, M., Yoshioka, Y., Ishida, T., Nakagawa, S. *et al*. Intravenous Administration of Polyethylene Glycol-Coated (PEGylated) Proteins and PEGylated Adenovirus Elicits an Anti-PEG Immunoglobulin M Response. *Biological & Pharmaceutical Bulletin* **35**, 1336-1342 (2012).

29 Zhang, P., Sun, F., Tsao, C., Liu, S., Jain, P. *et al*. Zwitterionic gel encapsulation promotes protein stability, enhances pharmacokinetics, and reduces immunogenicity. *Proceedings of the National Academy of Sciences* **112**, 12046-12051, doi:10.1073/pnas.1512465112 (2015).

30 Richter, A. W. & Akerblom, E. Antibodies against polyethylene-glycol produced in animals by immunization with monomethoxy polyethylene-glycol modified proteins. *International Archives of Allergy and Applied Immunology* **70**, 124-131 (1983).

31 Sherman, M. R., Williams, L. D., Sobczyk, M. A., Michaels, S. J. & Saifer, M. G. P. Role of the Methoxy Group in Immune Responses to mPEG-Protein Conjugates. *Bioconjugate Chemistry* **23**, 485-499, doi:10.1021/bc200551b (2012).

32 Saifer, M. G. P., Williams, L. D., Sobczyk, M. A., Michaels, S. J. & Sherman, M. R. Selectivity of binding of PEGs and PEG-like oligomers to anti-PEG antibodies induced by methoxyPEG-proteins. *Molecular Immunology* **57**, 236-246, doi:10.1016/j.molimm.2013.07.014 (2014).

CHAPTER 2

DESIGN AND SYNTHESIS OF ZWITTERIONIC POLYMERS FOR BIOCONJUGATION

Sijun Liu and Shaoyi Jiang

Abstract

Zwitterionic polymers have attractive properties for therapeutic applications, such as their ability to resist protein absorption and enable long circulation. However, current polymerization methods need to be updated to produce polymers without interfering species. Thus, we designed and synthesized a library of zwitterionic polymers with different sizes and functional groups for bioconjugation, using reversible addition-fragmentation chain-transfer polymerization.

2.1 Introduction

Zwitterions are molecules containing equal numbers of cationic and anionic groups, resulting in net neutral charge. Polymers of zwitterions can be naturally occurring, the most well known example being peptides and proteins made of zwitterionic amino acids. Glycine, one of the simplest amino acids, has an *N*-methylated analogue called trimethylglycine (TMG) or glycine betaine, a common molecule synthesized by organisms as an osmoprotectant against extreme osmotic stress.[1] Many other biologically relevant molecules are zwitterionic, such as phospholipids found in cell membranes and metabolites trigonelline and homarine.

In recent years, polymers of TMG analogues received significant interest as they have demonstrated valuable properties. Due to repeating units of charged groups, polyzwitterions are extremely hydrophilic and exhibit high resistance against nonspecific adsorption of biomacromolecules, referred to as nonfouling properties. A polymerizable analogue of TMG is carboxybetaine methacrylate (CBMA, **Scheme 2-1**), which is the focus of many material formulations, such as hydrogels, nanoparticles, surface coatings, and bioconjugates[2-15], due to its status as the best analogue studied[16]. Past experiments showed that poly(CBMA) surfaces are ultra-low fouling, where the adsorbed protein content was fewer than 0.3 ng/cm^2, and this property is retained in nanoparticle and hydrogel platforms: pCBMA nanoparticles resist opsonization in whole blood[5,8,13,14] and implanted pCBMA-covered medical devices inhibited capsules that normally form as part of the foreign body response[7].

One field of continuing investigation is the preparation of protein-polymer conjugates. Macromolecular therapeutics are fragile and sensitive to a variety of environmental factors, often requiring a delivery vehicle to protect and ensure survival post administration. The industry-standard conjugation polymer is poly(ethylene glycol), or PEG, which is a polymer of ethylene oxide (Scheme 2-1**)**. It has similar nonfouling properties as polyzwitterionic polymers, but it is nonionic and amphiphilic, allowing it to dissolve in a variety of organic and aqueous solvents. There is a growing need to replace PEG, as despite its ease of synthesis and apparent biocompatibility, reports show increasing incidence of PEG-specific antibodies and other host responses.[17] It is also known to interfere with active sites of proteins, possibly due to interactions between the PEG backbone and hydrophobic residues. A previous study of a pCBMA conjugate demonstrated the benefits afforded by the hydrophilic

polymer without common problems seen in PEG: it enhanced the stability of the underlying enzyme chymotrypsin without sacrificing bioactivity or binding affinity.[18,19] The current hypothesis is CBMA contains the most stable and bioactive monovalent ions and its polymer can strengthen protein structure while promoting specific binding at the hydrophobic binding site, which is similar to how certain ions naturally stabilize proteins[16].

In order to translate this work into therapeutic formulations, pCBMA platforms must be investigated in vivo. However, the current synthesis routes of pCBMA rely on copper-mediated atom-transfer radical polymerization and extraneous copper may negatively impact the homeostasis and health of study animals. Reversible addition-fragmentation chain-transfer polymerization (RAFT) is a technique capable of generating polymers with well-controlled molecular weights while allowing the facile introduction of various end groups through the aminolysis of the terminal Z group.[20] Further more, we utilized another analogue to TMG with more hydrophilic properties, by exchanging the MA group with an acrylamide group and forming carboxybetaine acrylamide (CBAAm). With these two changes, we designed and synthesized a library of pCBAAm polymers with varying sizes and functional groups for future bioconjugates studies.

2.2 Materials and methods

2.2.1 Materials

All chemicals and materials were supplied by Sigma-Aldrich (St. Louis, MO) unless otherwise specified. Methoxy-PEG-COO-NHS (NHS-mPEG, 10k MW) was purchased from NOF America Corporation (White Plains, NY). *N-a*-maleimidoacet-oxysuccinimide ester (AMAS) was purchased from Thermo Fisher Scientific (Waltham, MA). Spectra/Por regenerated cellulose dialysis membranes were purchased from Spectrum Laboratories, Inc (Rancho Dominguez, CA). Amicon Ultra centrifugal filter units were purchased from EMD Millipore (Billerica, MA).

2.2.2 Synthesis of the monomer 3-acrylamido-N-(2-(tert-butoxy)-2-oxoethyl)-N,N-dimethylpropan-1-aminium (tBu-CBAAm)

The synthesis route is summarized in

Scheme 2-2. In a 1-L round-bottom (RB) flask fitted with a stir bar, *N,N*-dimethylaminopropyl acrylamide (**1**, 60.01 g, 0.384 mol, 1 eq), *tert*-butyl bromoacetate (85.1 mL, 0.576 mol, 1.5 eq), and hydroquinone (500 mg as a polymerization inhibitor) were dissolved in acetonitrile (350 mL). The reaction mixture was stirred in a 60 °C oil bath for 12 h and then cooled to room temperature (RT). The product (**2**) was then precipitated in diethyl ether, filtered via a medium-porosity glass-fritted Buchner funnel, and dried under vacuum overnight to yield a white powder.

Yield: 98%. Proton ^{1}H NMR (300 MHz, $CDCl_3$, **Figure 2-1**) δ (ppm): 8.13 (t, *J* = 5.6 Hz, 1H), 6.35 (dd, *J* = 17.0, 10.2 Hz, 1H), 6.13 (dd, *J* = 17.0, 1.5 Hz, 1H), 5.48 (dd, *J* = 10.2, 1.5 Hz, 1H), 4.34 (s, 2H), 4.02-3.79 (m, 2H), 3.40 (s, 6H), 3.32 (d, *J* = 5.7 Hz, 2H), 2.15-1.93 (m, 2H), 1.37 (s, 9H).

2.2.3 Synthesis of SH-terminated poly(carboxybetaine acrylamide) (pCBAAm-SH)

The synthesis route is summarized in **Scheme 2-3**. In a typical reversible addition-fragmentation chain-transfer (RAFT) polymerization reaction to yield a 10-kDa polymer, 2-(dodecylthiocarbonothioylthio)-2-methylpropionic acid (DMP, 100 mg, 0.27 mmol, 1 eq), *tBu*-CBAAm (6.745 g, 19.2 mmol, 70 eq), 2,2'-azobis(2-methylpropionitrile) (AIBN, 8.9 mg, 0.054 mmol, 0.2 eq) were dissolved in anhydrous dimethylformamide (DMF, 35 mL) in a 100-mL round-bottom flask fitted with a stir bar. The flask was sealed with a rubber septum and sparged with N_2 for 30 min, then stirred in a 70 °C oil bath for 4 h. The resultant polymer **2** was precipitated in ice-cold ethyl acetate three times, centrifuged to pellet polymer, and dried under vacuum over night to yield a faintly yellow solid. For a typical aminolysis reaction, polymer **2** (995.0 mg), tris(2-carboxyethyl)phosphine hydrochloride (TCEP, 86.2 mg, 0.301 mmol, 1.5 eq), triethylamine (280 µL, 2.009 mmol, 10 eq), and hexylamine (264 µL, 1.998 mmol, 10 eq) were dissolved in anhydrous DMF (3 mL) for the removal of the trithiocarbonate group. After stirring at RT for 5 h, the product was precipitated in ice-cold diethyl ether, centrifuged, and dried under vacuum over night to yield a colorless solid, polymer **3**. The zwitterionic polymer **4** was obtained as a colorless solid by deprotecting the tBu groups of polymer **3** with trifluoroacetic acid (TFA, ~2 mL per 1 g polymer, ~10 eq) for 3 h at RT, followed by precipitation in ice-cold ethyl acetate, centrifugation, and drying under vacuum for 48 h.

To synthesize a 5-kDa polymer, the feed ratio of DMP to *tBu*-CBAAm is adjusted to 1:44 and reacted for 1 h 45 min while following the same procedure throughout the rest of the synthesis.

5,5'-dithio-bis(2-nitrobenzoic acid) (Ellman's reagent) was used to confirm the presence of thiol groups.

2.2.4 Synthesis of N-hydroxysuccinimide ester-functionalized pCBAAm (pCBAAm-NHS)

The synthesis route is summarized in **Scheme 2-4**. The zwitterionic polymer pCBAAm-SH previously described is activated by reaction with AMAS at 1:10 molar ratio in DI water (pH 6) for 30 min, followed by removal of unreacted AMAS via Amicon spin dialysis tubes and freeze-drying for 48 h.

2.2.5 Synthesis of the chain transfer agent tert-butyl (2-(2-(((dodecylthio)carbonothioyl)thio)-2-methylpropanamido)ethyl)carbamate (N-Boc-DMP)

The synthesis route is summarized in **Scheme 2-5**. In a rubber-stoppered 250-mL RB flask with stir bar, 2-(Dodecylthiocarbonothioylthio)-2-methylpropionic acid *N*-hydroxysuccinimide ester (**2**, 1.13 g, 2.45 mmol, 1.1 eq) was dissolved in 20 mL anhydrous dichloromethane. The flask was placed in a low-form 500-mL vacuum flask containing ethanol and dry ice was added until the ethanol bath dropped to below -20 °C. In a separate rubber-stoppered 100-mL RB flask, *N*-Boc-ethylenediamine (**1**, 0.36 g, 2.25 mmol, 1 eq) and triethylamine (0.25 g, 2.47 mmol, 1.1 eq) were dissolved in 10 mL anhydrous dichloromethane and delivered via syringe into solution **2**. The reaction was stirred for 12 h while the ethanol bath was manually kept to ≤20 °C with dry ice, then transferred to a 250-mL separatory funnel for 3x deionized water wash and 1x brine wash to remove unreacted water-soluble agents. The organic phase was dried with sodium sulfate for 1 h at RT, filtered to remove the insoluble salt, and fractionated on a silica gel column on a Isco Chromatography system (Teledyne Technologies, Thousand Oaks, CA) using a mixture of ethyl acetate and hexane (ramping over 45 min from 0% to 15% EtoAc). The fractions containing the product **3** were combined, rotovapped, and further dried under vacuum for 48 h.

Yield: 94%. Proton ^{1}H NMR (300 MHz, $CDCl_3$, **Figure 2-2**) δ (ppm): 6.91 (s, 1H), 4.85 (s, 1H), 3.28 (dt, *J* = 14.8, 6.7 Hz, 6H), 1.68 (s, 6H), 1.46-1.34 (m, 11H), 1.31-1.18 (m, 18H), 0.85 (t, *J* = 6 Hz, 3H).

2.2.6 Synthesis of NH_2-terminated pCBAAm (NH_2-pCBAAm)

Polymers were synthesized via the same route as pCBAAm-SH, but *N*-Boc-DMP was used as the CTA instead of DMP. The feed ratio remained 5:1 for CTA:AIBN, 1:44 CTA:monomer for 5-kDa polymers, and 1:70 CTA:monomer for 10-kDa polymers. 2,4,6-trinitrobenzene sulfonic acid (TNBSA) was used to quantify the presence of primary amines.

2.2.7 Analyses via size-exclusion chromatography

All samples were processed in a 1260 Infinity binary high performance liquid chromatography (HPLC) system equipped with a UV detector (Agilent Technologies, Santa Clara, CA), a miniDAWN TREOS multi-angle light scattering (MALS) detector, and a Optilab T-rEX differential refractive index (dRI) detector (Wyatt Technology, Santa Barbara, CA). The flow rate was set at 1 mL/min with the mobile phase PBS (pH 7.4) with 0.02% sodium azide added as a preservative. Polymers were fractionated in a Waters Ultrahydrogel 1000 column (7.8 mm x 300 mm, 12 μm particle size). Absolute molecular weight (MW) of PCB polymers were calculated using dn/dc values determined using the ASTRA software (Wyatt Technology, Santa Barbara, CA) via batch-mode injections of known mass concentrations. MW with respect to polyethylene glycol (PEG) was determined by generating a standard curve with six PEG samples of known MW and polydispersity (PDI, M_n/M_w).

2.3 Results and discussions

2.3.1 PEG-equivalent pCBAAm polymers

PCBAAm, with its zwitterionic side chains, is structurally very different from PEG, making a direct comparison difficult. If a pCBAAm polymer has the same absolute molecular weight (M_n) as PEG, it is actually smaller in solution. However, as PEG is the industry standard, it is more convenient to have pCBAAm polymers that are the same hydrodynamic size (M_{Rh}) as PEG. For this reason, we chose 5

kDa and 10 kDa as target sizes, as they are the most utilized PEG sizes for conjugation to protein therapeutics. As seen in the size-exclusion chromatograms in **Figure 2-3**, the PEG-equivalent sizes of pCBAAm were achieved. The peaks were broader than PEG, i.e. slightly more polydisperse, but that is a common result of polyacrylamide polymerization. This is corroborated by the polydispersity index (PDI), where pCBAAm polymers have PDI <1.2, which is considered monodisperse for polymer applications.[21] **Table 2-1** summarizes the PDI and other physical parameters of pCBAAm polymers and their target PEG counterparts.

2.3.2 Confirmation of functional groups

We have synthesized pCBAAm polymers with three different types of terminal functional groups, but we need to confirm their presence. Fortunately, they are well-studied end groups and thus quantification methods already exist. We were able to use the Ellman reagent to detect thiols, TNBSA for primary amines, and UV-VIS for NHS esters. The results are summarized in **Table 2-2**.

2.4 Conclusions

We successfully synthesized pCBAAm polymers with hydrodynamic sizes equivalent to PEG with low polydispersity. They have terminal functional groups that are widely used in bioconjugation: NHS ester-activated carboxyl group, thiol group, and primary amine group. These were synthesized without the addition of copper, and is thus ready to be used for modification of therapeutically relevant proteins.

2.5 Acknowledgments

We would like to thank the National Institutes of Health for generously funding this work through its T32 Predoctoral Training grant (T32A138312) and Dr. Andrew J. Keefe for interesting discussions regarding his original design of the pCBMA polymers.

2.6 Figures, schemes, and tables

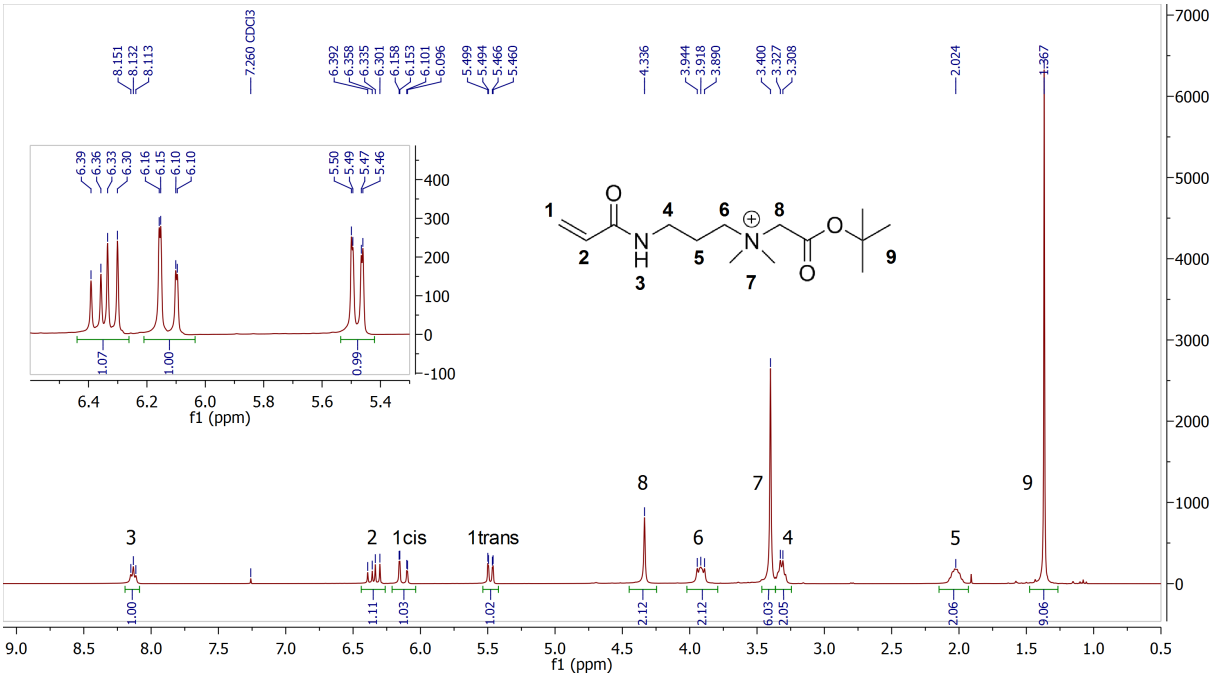

Figure 2-1: Proton NMR spectrum of CBAAm-1-tBu (300 MHz, $CDCl_3$). Inset shows the acrylamide proton peaks.

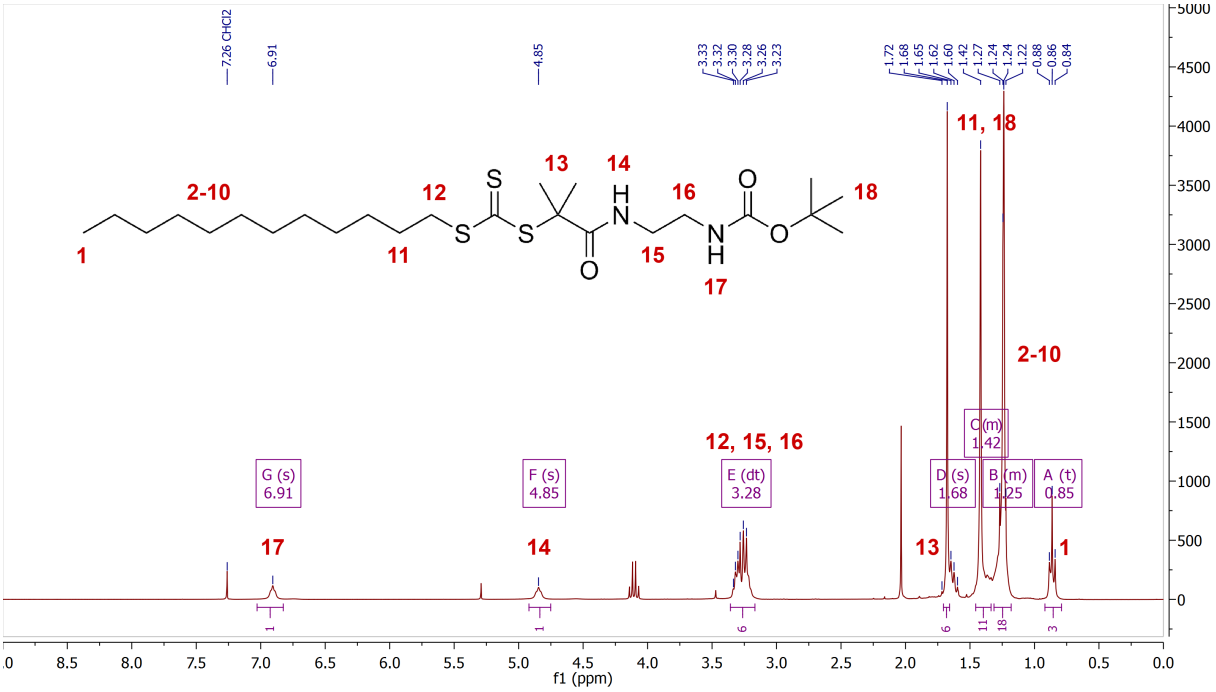

Figure 2-2: Proton NMR spectrum of *N*-Boc-DMP (300 MHz, $CDCl_3$).

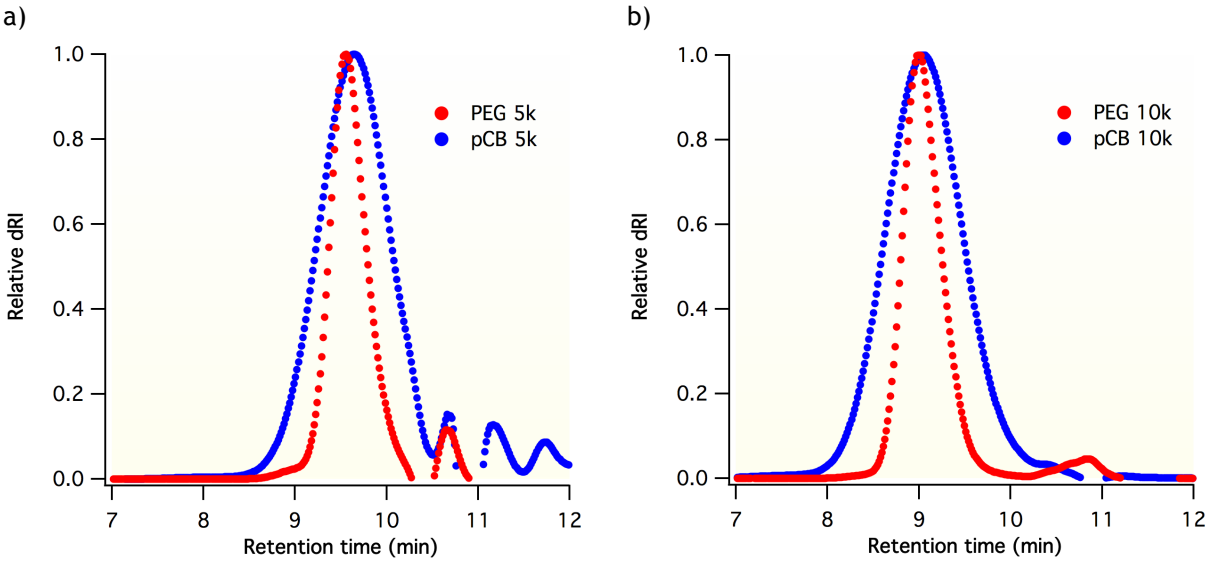

Figure 2-3: SEC chromatograms of pCBAAm polymers with molecular weights comparable to PEG via hydrodynamic size. The targetd pCB sizes were a) 5 kDa and b) 10 kDa.

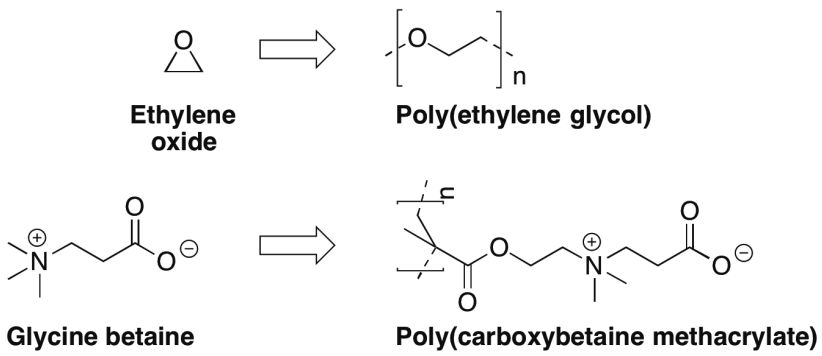

Scheme 2-1: Structures of ethylene oxide and glycine betaine, as well as their polymers poly(ethylene glycol) and poly(carboxybetaine methacrylate).

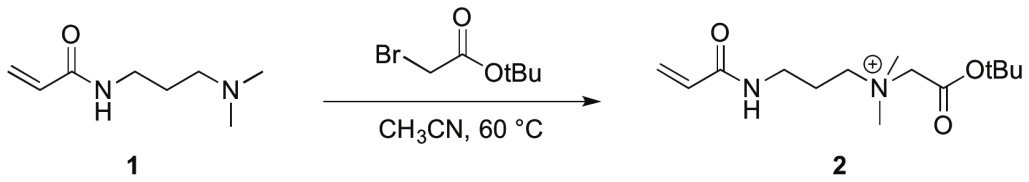

Scheme 2-2: Synthesis of tBu-CBAAm.

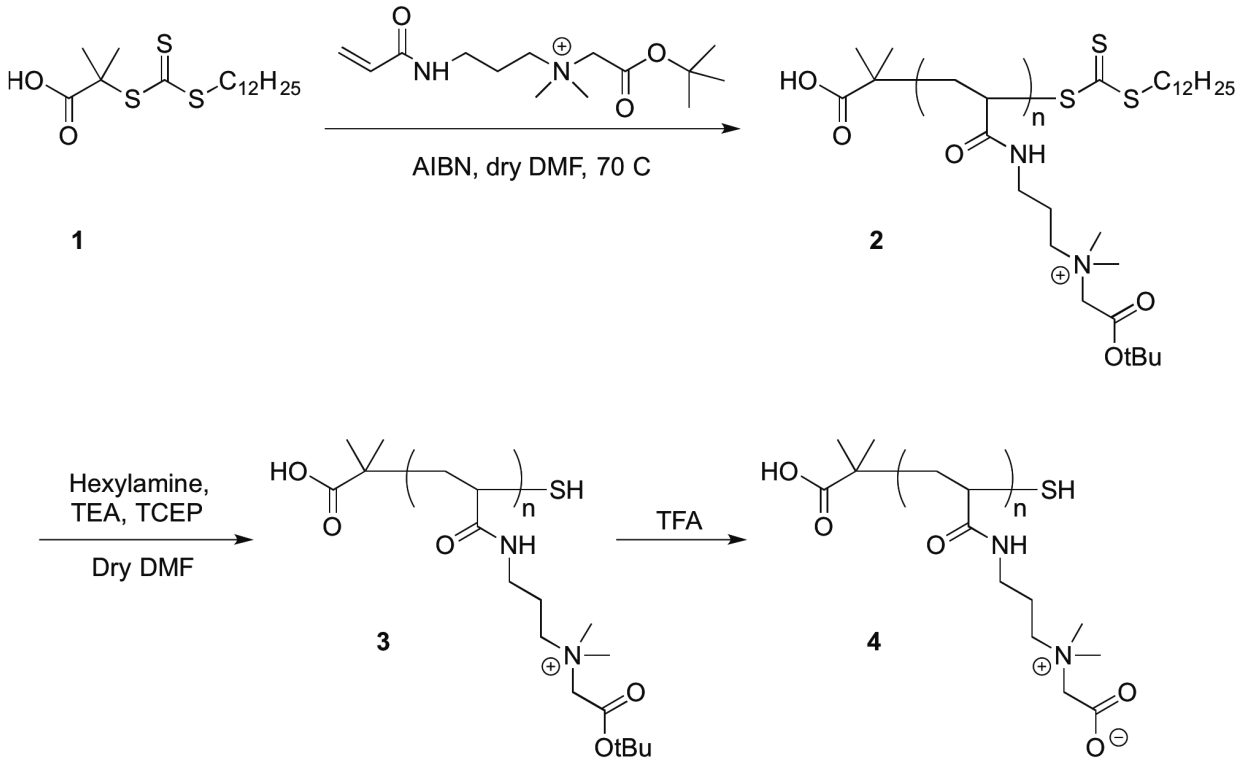

Scheme 2-3: Synthesis of pCBAAm-SH.

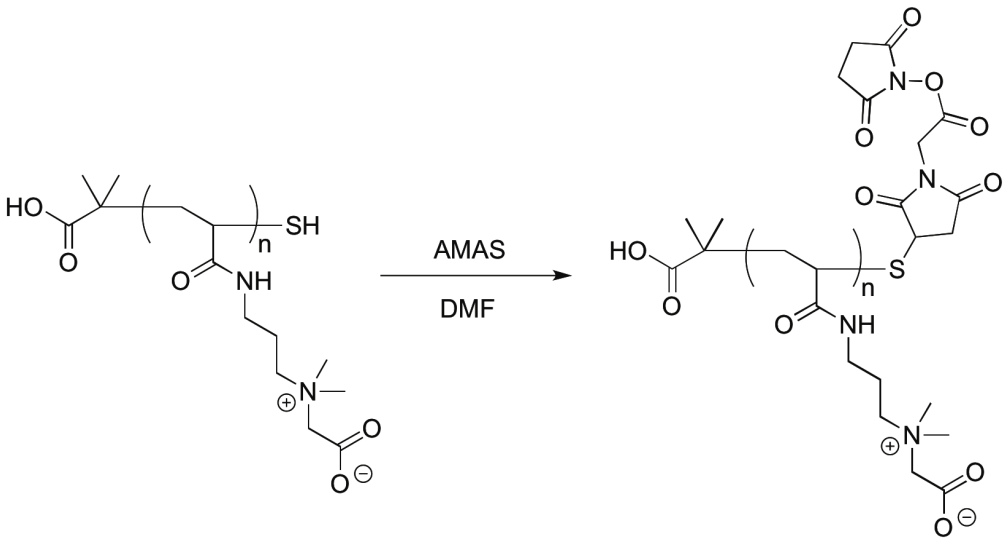

Scheme 2-4: Synthesis of pCBAAm-NHS.

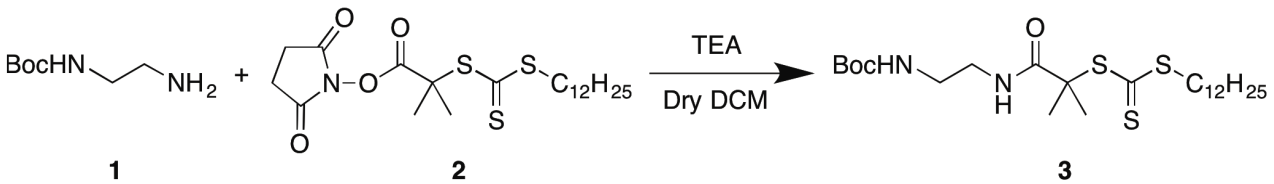

1 2 3

Scheme 2-5: Synthesis of *N*-Boc-DMP.

Table 2-1: Absolute molecular weight (M_n) and PEG-equivalent hydrodynamic size (M_{Rh}) of representative pCBAAm polymers.

		MW (kDa)	PDI (M_w/M_n)
5 kDa	SEC (absolute MW)	11.7	1.11
	SEC (PEG standards)	5.2	N/A
10 kDa	SEC (absolute MW)	21	1.13
	SEC (PEG standards)	9.9	N/A

Table 2-2: Results from confirmation of terminal groups for a representative 10 kDa (R_h MW) polymer.

Terminal group	#/polymer chain
SH	1.1
NH_2	1.3
NHS ester	0.9

2.7 References

1 Neuhofer, W. & Beck, F. X. Survival in hostile environments: Strategies of renal medullary cells. *Physiology* **21**, 171-180, doi:10.1152/physiol.00003.2006 (2006).

2 Zhang, P., Sun, F., Tsao, C., Liu, S., Jain, P. *et al*. Zwitterionic gel encapsulation promotes protein stability, enhances pharmacokinetics, and reduces immunogenicity. *Proceedings of the National Academy of Sciences* **112**, 12046-12051, doi:10.1073/pnas.1512465112 (2015).

3 Liu, S. & Jiang, S. Zwitterionic polymer-protein conjugates reduce polymer-specific antibody response. *Nano Today* **11**, 285-291 (2016).

4 Yang, W., Liu, S., Bai, T., Keefe, A. J., Zhang, L. *et al*. Poly(carboxybetaine) nanomaterials enable long circulation and prevent polymer-specific antibody production. *Nano Today* **9**, 10-16, doi:10.1016/j.nantod.2014.02.004 (2014).

5 Yang, W., Ella-Menye, J.-R., Liu, S., Bai, T., Wang, D. Q. *et al*. Cross-Linked Carboxybetaine SAMs Enable Nanoparticles with Remarkable Stability in Complex Media. *Langmuir* **30**, 2522-2529, doi:10.1021/la404941m (2014).

6 Bai, T., Liu, S., Sun, F., Sinclair, A., Zhang, L. *et al*. Zwitterionic fusion in hydrogels and spontaneous and time-independent self-healing under physiological conditions. *Biomaterials* **35**, 3926-3933, doi:10.1016/j.biomaterials.2014.01.077 (2014).

7 Zhang, L., Cao, Z. Q., Bai, T., Carr, L., Ella-Menye, J. R. *et al*. Zwitterionic hydrogels implanted in mice resist the foreign-body reaction. *Nature Biotechnology* **31**, 553-+, doi:10.1038/nbt.2580 (2013).

8 Zhang, L., Cao, Z. Q., Li, Y. T., Ella-Menye, J. R., Bai, T. *et al*. Softer Zwitterionic Nanogels for Longer Circulation and Lower Splenic Accumulation. *Acs Nano* **6**, 6681-6686, doi:10.1021/nn301159a (2012).

9 Zhang, L., Xu, J. J., Mi, L., Gong, H., Jiang, S. *et al*. Multifunctional magnetic-plasmonic nanoparticles for fast concentration and sensitive detection of bacteria using SERS. *Biosensors & Bioelectronics* **31**, 130-136, doi:10.1016/j.bios.2011.10.006 (2012).

10 Keefe, A. J. & Jiang, S. Poly(zwitterionic)protein conjugates offer increased stability without sacrificing binding affinity or bioactivity. *Nature Chemistry* **4**, 60-64, doi:10.1038/nchem.1213 (2012).

11 Cao, Z. Q., Zhang, L. & Jiang, S. Superhydrophilic Zwitterionic Polymers Stabilize Liposomes. *Langmuir* **28**, 11625-11632, doi:10.1021/la302433a (2012).

12 Zhang, L., Xue, H., Cao, Z. Q., Keefe, A. J., Wang, J. N. *et al*. Multifunctional and degradable zwitterionic nanogels for targeted delivery, enhanced MR imaging, reduction-sensitive drug release, and renal clearance. *Biomaterials* **32**, 4604-4608, doi:10.1016/j.biomaterials.2011.02.064 (2011).

13 Cheng, G., Mi, L., Cao, Z. Q., Xue, H., Yu, Q. M. *et al*. Functionalizable and Ultrastable Zwitterionic Nanogels. *Langmuir* **26**, 6883-6886, doi:10.1021/la100664g (2010).

14 Cao, Z. Q., Yu, Q. M., Xue, H., Cheng, G. & Jiang, S. Nanoparticles for Drug Delivery Prepared from Amphiphilic PLGA Zwitterionic Block Copolymers with Sharp Contrast in Polarity between Two Blocks. *Angewandte Chemie-International Edition* **49**, 3771-3776, doi:10.1002/anie.200907079 (2010).

15 Jia, G. W., Cao, Z. Q., Xue, H., Xu, Y. S. & Jiang, S. Novel Zwitterionic-Polymer-Coated Silica Nanoparticles. *Langmuir* **25**, 3196-3199, doi:10.1021/la803737c (2009).

16 Shao, Q. & Jiang, S. Y. Molecular Understanding and Design of Zwitterionic Materials. *Advanced Materials* **27**, 15-26, doi:10.1002/adma.201404059 (2015).

17 Yang, Q. & Lai, S. K. Anti-PEG immunity: emergence, characteristics, and unaddressed questions. *Wiley Interdisciplinary Reviews-Nanomedicine and Nanobiotechnology* **7**, 655-677, doi:10.1002/wnan.1339 (2015).

18 Veronese, F. M. & Harris, J. M. Peptide and protein PEGylation III: advances in chemistry and clinical applications. *Advanced Drug Delivery Reviews* **60**, 1-2, doi:10.1016/j.addr.2007.08.003 (2008).

19 Fishburn, C. S. The pharmacology of PEGylation: Balancing PD with PK to generate novel therapeutics. *Journal of Pharmaceutical Sciences* **97**, 4167-4183, doi:10.1002/jps.21278 (2008).

20 Willcock, H. & O'Reilly, R. K. End group removal and modification of RAFT polymers. *Polymer Chemistry* **1**, 149-157, doi:10.1039/b9py00340a (2010).
21 Nobbmann, U. *Polydispersity – what does it mean for DLS and chromatography?*, <http://www.materials-talks.com/blog/2014/10/23/polydispersity-what-does-it-mean-for-dls-and-chromatography/> (2014).

CHAPTER 3

CHEMICAL CONJUGATION OF ZWITTERIONIC POLYMERS PROTECTS IMMUNOGENIC ENZYME AND PRESERVES BIOACTIVITY WITHOUT POLYMER-SPECIFIC ANTIBODY RESPONSE

Sijun Liu and Shaoyi Jiang

Abstract

Proteins are promising therapeutics with several design challenges, such as their inherent immunogenicity due to their exogenous source or short circulation time. The common solution to such issues is the chemical conjugation of the amphiphilic polymer poly(ethylene glycol) (PEG), a process known as PEGylation. However, several studies demonstrated a decrease in protein bioactivity or an increase in the presence of specific antibodies post PEGylation, highlighting the importance of an alternative strategy. Here we compare the performance of a superhydrophilic zwitterionic polymer in protecting an immunogenic protein to PEG in (i) the maintenance of enzyme activity and stability post modification, (ii) mitigation of the antibody response elicited by the polymer and any subsequent effect on pharmacokinetics, and (iii) minimization of host response toward the underlying protein. In contrast to PEG, zwitterionic conjugation decreases host antibody response without sacrificing bioactivity or generating polymer-specific antibodies.

3.1 Introduction

Proteins play critical and diverse roles in the normal function of the body, which makes them excellent candidates as therapeutics to alleviate diseases not easily treated with simple chemical drugs. However, this line of treatment is not without its shortcomings. Proteins as a macromolecule present many stability issues, both during their manufacturing and subsequent usage in the body: their aggregation is often a problem and various host defense mechanisms usually rapidly remove them from circulation. In some cases of exogenous protein therapeutics, the body even mounts an efficient immune response to cleanse them prematurely from the system and thus lowering the efficacy or increasing the dosage necessary to achieve the desired response.[1-3]

The chemical conjugation of the synthetic polymer polyethylene glycol (PEG) has been the solution of the industry to these challenges, albeit an imperfect one. The addition of PEG, or PEGylation, provides bulk while conferring a protective layer: this often mitigates clearance mechanisms that rely on filtering of smaller sizes or recognition due to nonspecific adsorption of serum proteins.[4] However, PEGylation adds another complexity, as multiple studies demonstrated a decrease in protein activity[5,6], as well as an apparent antigenicity[7-11] of PEG. Much like a hapten, PEG becomes immunogenic once conjugated to a large protein and initiates antibody generation in many animal models as well as humans.[7-10,12-14] This translates to a compromise between the positive protection afforded by PEG and the increased immunogenicity of the final overall therapeutic product. In some systems, the former may not outweigh the problems introduced by the latter.

In contrast to the amphiphilic PEG, zwitterionic polymers based on naturally occurring betaines are entirely hydrophilic and confer the same protection without the complicating negative traits. Each polymer contains the same number of positively and negatively charged groups, thus maintaining an overall neutral charge, much like many proteins. These polymers as components of nanoparticles (NPs) demonstrated excellent long-circulation abilities, often yielding half-lives multiple times longer than the equivalent PEG NP.[15-22] At the same time, polymer-specific antibodies were absent, while anti-PEG antibodies were clearly detected and quantified.[21,22] Furthermore, protein conjugates studied *in vitro* showed maintenance or improved stability of the underlying protein without reducing bioactivity or binding affinity.[23] Combining these encouraging results, we designed a protein conjugate system to

study the effect of zwitterionic polymers on enzyme activity, pharmacokinetics, and immunogenicity, with native and PEGylated proteins as comparison.

The model protein chosen for this study is uricase, which is an FDA-approved treatment for refractory gout. However, uricase is by definition a foreign protein and thus highly immunogenic. While PEGylated uricase reduced host response toward the protein, it instead raised neutralizing antibodies toward PEG, which still negatively affected the in vivo pharmacokinetics of the conjugate.[24,25] Thus, this protein system presents an area where we can directly compare to a commercial conjugate that improved upon the performance of the bare protein, but is an insufficient solution to the problem.

We aim to address three questions regarding protein conjugation with zwitterionic poly(carboxybetaine acrylamide) (PCB): (i) can it retain native activity post protein modification, (ii) does the superhydrophilic polymer generate any specific antibody response toward itself like PEG does, and (iii) can polyzwitterions protect the underlying enzyme as well as the PEG counterpart? An extensive study in the rat animal model provides antisera generated in response to bare protein, PEGylated protein, and polyzwitterion-conjugated protein, which yields both antibody data and enzyme activity measurements. The collected findings offer encouraging support for polyzwitterions as the next generation of non-immunogenic polymers for the protection of exogenous protein therapeutics via chemical conjugation.

3.2 Materials and methods

3.2.1 Materials

All chemicals (unless otherwise specified) and recombinant uricase from *Candida sp.* expressed in *E. coli* were purchased from Sigma-Aldrich (St. Louis, MO). Methoxy-PEG-COO-NHS (NHS-mPEG, 10k MW) was purchased from NOF America Corporation (White Plains, NY). Amplex Red Uricase Assay kits, Costar 96-well EIA/RIA plates, and Pierce Protein Concentrators (150k MWCO) were purchased from Thermo Fisher Scientific (Waltham, MA). Male and female Sprague Dawley rats were purchased from Charles River Laboratories (Burlington, MA). Sterile 0.22 μm Millex-GP syringe filters and Amicon Ultra centrifugal filter units were purchased from EMD Millipore (Billerica, MA). Spectra/Por regenerated cellulose dialysis membranes were purchased from Spectrum Laboratories, Inc (Rancho Dominguez,

CA). Antibodies were purchased from Abcam (Massachusetts, US). 3,3',5,5'-Tetramethylbenzidine (TMB) substrate solution was purchased from eBioscience (San Diego, CA).

3.2.2 Syntheses of polymer-protein conjugates

In a typical conjugation reaction, uricase (26.8 mg, 0.19 μmol) and NHS ester-functionalized PCB (190.6 mg, 9.5 μmol, 50 eq) were dissolved in phosphate-buffered saline (PBS, pH 7.4) and immediately combined (final concentration of 10 mg/mL protein). The reaction mixture was gently shaken at RT for 1 h, following by removal of unreacted reagents via 150-kDa molecular weight cut-off (MWCO) spin dialysis membrane. The same conjugation and purification methods were used to generate PEGylated uricase and rat serum albumin (RSA) using NHS-mPEG, as well as polyzwitterion-conjugated RSA.

3.2.3 Analyses via size-exclusion chromatography (SEC)

All samples were processed in a 1260 Infinity binary high performance liquid chromatography (HPLC) system equipped with a UV detector (Agilent Technologies, Santa Clara, CA), a miniDAWN TREOS light scattering (LS) detector, and a Optilab T-rEX differential refractive index (dRI) detector (Wyatt Technology, Santa Barbara, CA). The flow rate was set at 1 mL/min with the mobile phase PBS (pH 7.4) with 0.02% sodium azide as a preservative. Polymers were fractionated in an Agilent PL aquagel-OH 20 column (7.5 mm x 300 mm, 8 μm particle size) while a Waters Ultrahydrogel 1000 column (7.8 mm x 300 mm, 12 μm particle size) was used for polymer-protein conjugates. Absolute molecular weight (MW) of PCB polymers were calculated using a dn/dc value determined using the ASTRA software (Wyatt Technology, Santa Barbara, CA) via batch mode injections of known concentrations. MW with respect to PEG was determined by generating a standard curve with six PEG samples of known MW and polydispersity index (M_n/M_w). The degree of polymer conjugation for each conjugate was calculated using the dn/dc values of the protein and polymer and the "Protein Conjugate" method supplied by the ASTRA software.

3.2.4 Stability assessment with respect to pH

Each protein formulation was incubated in 0.1 M sodium phosphate buffer adjusted to pH value of 5, 5.6, 6.2, 6.8, 7.4, 8, or 8.6 for 6 h at room temperature for 3 h. The Amplex Red Uricase Assay kits were used following manufacturer's instructions to ascertain specific activity of each formulation before and after treatment. The activity of the native uricase at pH 7.4 was set to 100% activity and all other values were normalized with respect to it.

3.2.5 Animal studies

The University of Washington Institutional Animal Care and Use Committee reviewed and approved all animal experiments under protocol #4203-01 prior to conducting studies. Male and female Sprague Dawley rats of ~150 g were randomly divided into groups of four (two each gender), one group each for bare enzyme, PEGylated uricase, and polyzwitterion-conjugated uricase. Weights were recorded at day 0 to ascertain the volume of administration for formulations of 1 mg protein/mL PBS to be administered at 1 mg uricase per kg animal (

Figure 3-2). On the same day, baseline sera were generated from blood collected from each animal. On days 1, 8, 15, and 22, each enzyme formulation was administered into the rat tail vein under aseptic surgical conditions with isoflurane anesthesia. On days 6, 13, and 20, blood was collected from each animal to yield sera. On days 1-3 and 22-24, blood was sampled 5 min, 6 h, 24 h, 48 h, and 72 h post injection to generate the respective circulation profile of the different protein formulations as affected by possible antibody production. All blood samples were treated by allowing clotting to occur at room temperature for 30 min, centrifuged to pellet the cellular debris, and the clear supernatant was collected as serum samples and frozen in small aliquots until use.

3.2.6 Detection of anti-uricase and anti-polymer antibodies

Indirect enzyme-linked immunosorbent assay (ELISA) experimental conditions were developed to detect antibodies specific for uricase, PEG, or PCB. A capturing protein (uricase, PEG-RSA, or PCB-RSA) was first adsorbed onto the plate in carbonate/bicarbonate buffer (0.2 M, pH 9.4) at 1 μg enzyme/well for 2 h at RT. After 2x wash using PBS supplemented with 0.025% (w/v) digitonin, the plate was blocked with 5% nonfat dry milk solution in PBS overnight at 4 °C. After another 2x wash,

pooled serum samples along with controls were added in triplicate and incubated for 2 h at RT followed by 5x wash. Detection antibody (goat anti-rat IgM IgG or goat anti-rat IgG IgG) diluted 1:20,000 was then added and incubated at RT for 1 h. After 5x wash, TMB solution was added for 15 min and quenched with 2 N H_2SO_4 stop solution. The plates were measured for absorbance at 450 nm with 570 nm values as background subtraction. For the detection of uricase-specific antibodies, native uricase serum samples were used as positive control and pre-experiment blood samples were used as negative control. Polymer-specific antibody detection assays were further validated via competition with free PCB or PEG polymer. Anti-PEG IgM serum concentrations were quantified using commercial monoclonal rat anti-PEG IgM, which is also the positive control for the polymer-specific assays.

3.2.7 Determination of circulation profile

The Amplex Red Uricase Assay kits were used following manufacturer's instructions to ascertain specific activity of bare uricase and the uricase conjugates as a surrogate marker for blood concentration. The circulation plots were generated and the Igor Pro software was used to calculate the elimination half-life (ln 2/ß) and relative bioactivity (integral of circulation curve from zero to infinity) of each formulation by fitting the data to a two-phase exponential decay function that describes two-component pharmacokinetics, $C(t) = a \cdot e^{-\alpha t} + b \cdot e^{-\beta t}$.

3.3 Results and discussion

In order to generate a fair comparison between the PEGylated and polyzwitterionic conjugates, we designed the end protein-conjugate products to contain similar amounts of polymers with the same molecular weight (**Table 3-1**) via the same conjugation chemistry (**Figure 3-1**). This way, the study animals were exposed to similar content of each type of polymer.

3.3.1 Enzyme activity and stability in buffer with respect to pH

Functional uricase exist as a tetramer of about 140 kDa and the dissociation into subunits results in a decrease in enzyme activity. Some reports have also shown a decrease in activity due to polymer conjugation[5,6], possibly due to steric blockage of active sites. Therapeutic PEG-uricase has

been shown to retain most of its native activity with higher degree of conjugation, as its substrate is small and can diffuse readily. The PEG and zwitterionic conjugates synthesized in this study have shown similar levels of activity maintenance (>95%) with respect to the native protein after optimization of conjugation (Table 3-1). Size-exclusion chromatography analysis shows that each subunit of uricase reacted with similar numbers of PEG or zwitterionic polymer chains (Table 3-1) and the final conjugates are similar in hydrodynamic size (

Figure 3-3).

As the kidneys can vary pH from about 4.5 to 8.5 for the maintenance of blood pH between 7.38 and 7.42, stability of the enzyme formulations in that range is important to investigate as the proteins circulate through the body. Previously, uricase has been shown to demonstrate maximum activity around pH 8.5 to 9 and generally decreases with lower pH.[26] In **Figure 3-4**, we compared the retained activity of native uricase with the bioconjugates. All three types function relatively similarly around pH 7.4, but differences became prominent at higher and lower pH: native uricase loses more than 90% of its activity at physiological pH when the pH drops below its isoelectric point of 5.6, with little protection from PEGylation. However, the PCB conjugate retained more than three times the native activity. This could be due to the inherent differences between the amphiphilic PEG and the superhydrophilic PCB—as the protein loses its tertiary and quaternary structures due to pH-related loss in charge, the polyelectrolyte polymer better protected against dissociation and hence higher activity. Interestingly, the zwitterionic conjugate also showed higher activity than the native enzyme at high pH, a phenomenon that correlates well with previous in vitro report of polyzwitterion conjugation[23], where the K_m value (substrate affinity) decreased with increasing numbers of PCB polymers conjugated.

3.3.2 Polymer-specific antibody detection

Previous work has highlighted the presence of polymer-specific antibodies[7-10,13,14,21,22,24], which continued to mediate immune clearance in addition to any generated toward the protein itself. To detect and compare the possible antibodies generated against polyzwitterions vs. PEG, we prepared rat proteins conjugated with either polymer at similar densities. As the rat host tolerates the protein

itself, the only antibodies captured by these conjugates are directed toward the attached polymer. **Figure 3-5**a-b shows the PEG IgM titer is 81x (43,740) and the IgG titer is 243x (131,220) that of the corresponding PCB titers (540 for both). At the lowest dilution, zwitter-specific antibody signal is barely distinguishable from the baseline signal and is similar to the nonspecific adsorption control (**Table 3-2**), suggesting that the signal is within assay error and the concentration is too low to be concerning.

As rat anti-PEG IgM antibody is commercially available, we generated a standard curve to quantify PEG-specific titer. The results are summarized in

Figure 3-6, in which anti-PEG IgM steadily increased over the three-injection study period, yielding 8x more IgM in week 3 (368 μg/mL) than week 1 (46 μg/mL). An analogous quantification plot for anti-PCB antibody concentration was not possible because we could not detect it above background noise as previous described and no commercial anti-PCB antibody was available.

3.3.3 Protection of protein from immune recognition

As the native uricase used in this study is of yeast origin and expressed in *E. coli*, the mammalian immune system can easily recognize it as foreign and thus initiates numerous clearance mechanisms. A typical antibody-mediated response starts with the generation of IgM within 1-2 weeks of initial immunogen encounter, which escalates to more rapid responses upon multiple exposures of the same agent. At this time, isotype switching occurs and IgG antibodies become the dominant isotype, which can achieve significant titer within days. Thus, within our study system, we expect to see elevated IgM and IgG generated against the exotic uricase, but the presence of protective polymers on the bioconjugates may shield the underlying enzyme to some degree.

The dosage for all three enzyme formulations was 1 mg protein per kg animal weight, which is consistent with the clinical therapeutic dosage of uricase.[27] One week following three repeated weekly administrations of the native enzyme, protein-specific IgM antibody titer was 40,960. With the same dosing schedule, uricase-specific IgM titer was much lower in the bioconjugates: 5,120 for serum samples derived from animals that received PEG conjugates and 640 for zwitterionic conjugates (Figure 3-5c). As for IgG, the native enzyme elicited a titer of 393,660, while the conjugates were 14,580 for

PEG conjugate serum samples and 4,860 for PCB (Figure 3-5d). For both antibody isotypes, the animals receiving zwitterionic conjugates mounted the weakest response: 64x less IgM and 81x less IgG than the titer evoked by the native enzyme, as well as 8x less IgM and 9x less IgG than that elicited by PEGylated uricase. As control, all baseline serum samples tested negative for either isotype of anti-uricase antibodies.

3.3.4 Circulation profile affected by immunological responses

Due to the presence of protein- and/or polymer-specific antibodies, the pharmacokinetics of native enzyme or polymer conjugates will alter depending on immune clearance mechanisms. After repeated administration of the same immunogenic agent, the body becomes primed to efficiently eliminate the foreign substance and thus decrease its systemic circulation potential. In our study after three injections, the elimination half-life of native uricase is the shortest at 6.2 h from 13 h of the first injection, followed by PEG conjugates at 25.6 h from 37 h, while zwitterionic conjugates has the longest half-life at 78 h with almost no change (**Table 3-3**). The circulation profiles are summarized in Figure 4.

This correlates well with the antibody results. Bare uricase elicited the most amount of specific antibody generation and was thus the easiest to recognize and remove by the host immune system. PEGylated conjugates managed to shield some protein-specific response, but in turn boosted PEG's antigenicity and are eliminated via polymer-specific mechanisms in addition to those specific to the protein. Polyzwitterion-conjugated conjugates protected the underlying enzyme to a degree without generating any antibody response to the polymer; they performed the best by maintaining the longest circulation. The relative bioavailability, or the area under the circulation curve, of each enzyme or enzyme conjugate, further reflects this: zwitterionic conjugate leads with 10.2x that of native uricase and 3.6x fold increase over PEG conjugates (Table 3-3).

3.4 Conclusions

We evaluated polyzwitterions as a stealth layer that protects the underlying protein therapeutic from host immune recognition without sacrificing enzymatic activity or inducing polymer-

specific antibody production. Across relevant pH ranges, zwitterionic conjugates sustained higher activity, likely due to the stabilizing nature of the polymer that promoted higher substrate affinity. The polyzwitterion-conjugated enzyme also outperformed both the native protein and the current industry-standard PEGylated construct in decreasing protein-specific humoral responses with no detectable zwitter-specific antibodies, while increasing the circulation half-life and bioavailability of the enzyme post multiple administrations. This technology translates previously reported benefits afforded by polyzwitterions in nanoparticles to biologically relevant protein therapeutics. The encouraging results presented here highlight the potential of these biocompatible polymers in the protection and delivery of exogenous and thus immunogenic biologics for human medicine.

3.5 Acknowledgments

We gratefully acknowledge the funding agencies for supporting this work: National Institutes of Health (1R21EB020781-01 and T32A138312) and Defense Threat Reduction Agency (HDTRA1-13-1-0044). We would also like to thank Dr. Jean-René Ella-Menye for helpful discussions regarding organic synthesis.

3.6 Figures and tables

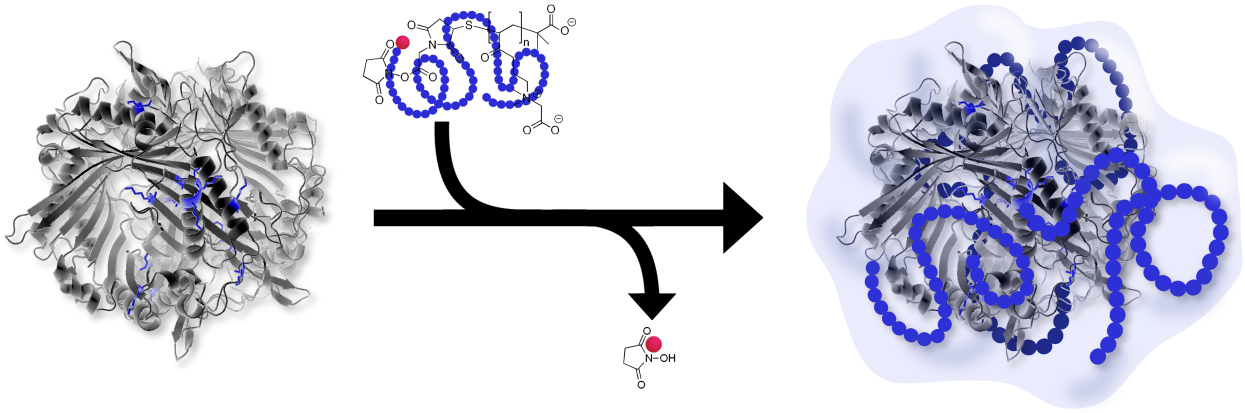

Figure 3-1: Conjugation of activated polymers results in a stealth shell around the enzyme.

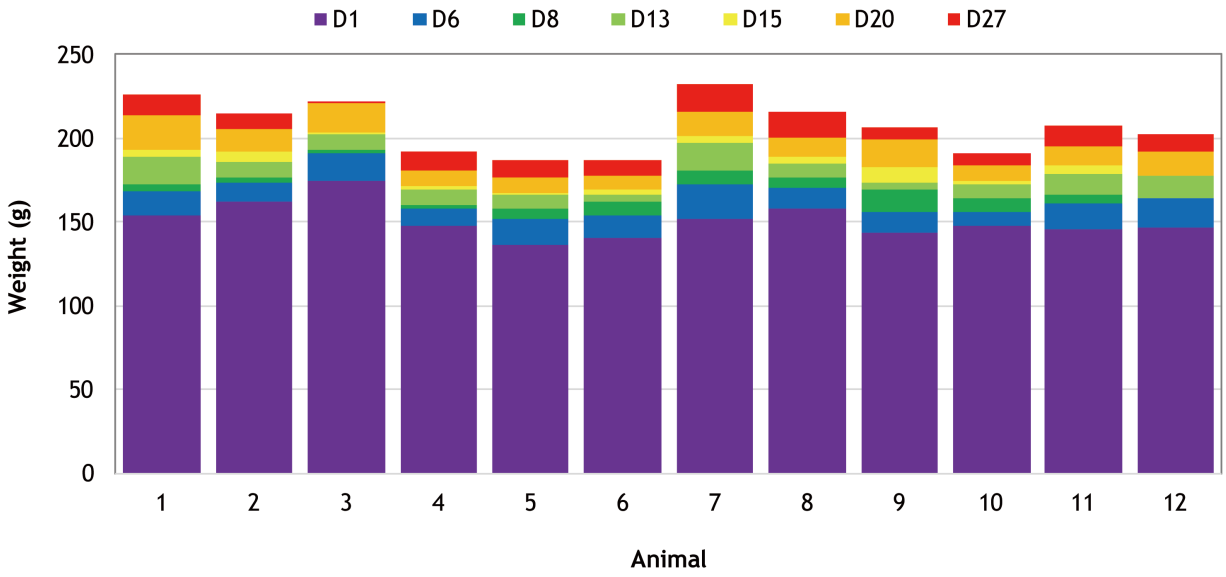

Figure 3-2: Weight records of the study animals over the length of the study.

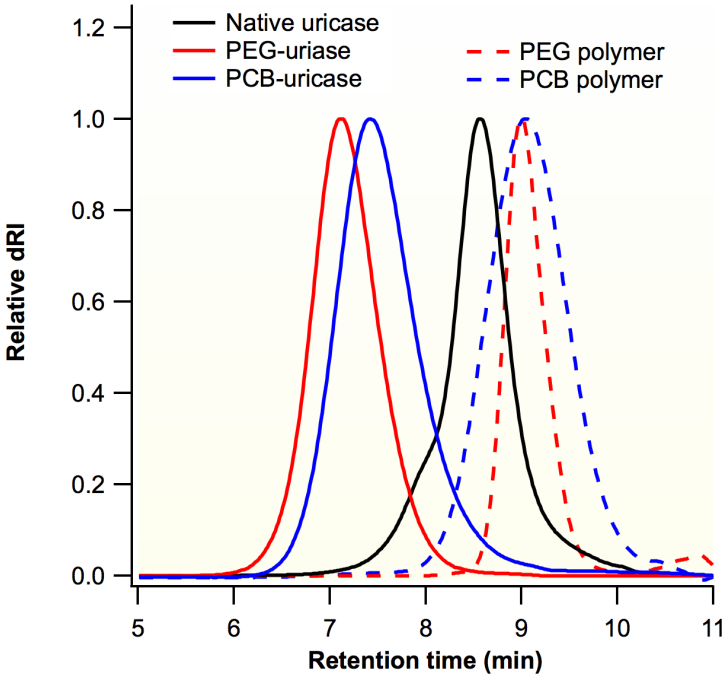

Figure 3-3: Size exclusion chromatogram of the polymers, native protein, and protein conjugates. In order to achieve a fair evaluation, molecular weight was designed to be comparable between PCB and PEG polymers, as well as between their subsequent protein conjugates. The SEC traces demonstrate the polymers are the same size and the protein conjugates are approximately the same.

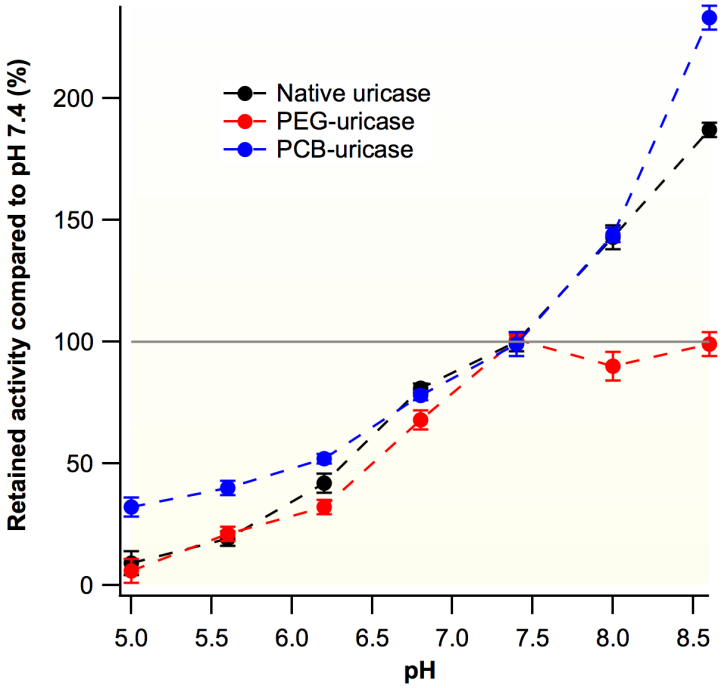

Figure 3-4: Bioactivity of uricase and uricase conjugates as a function of pH. The activity of native uricase at physiological pH was set to 100% and all other activity values were normalized accordingly. The error bars represent standard deviation across three replicates.

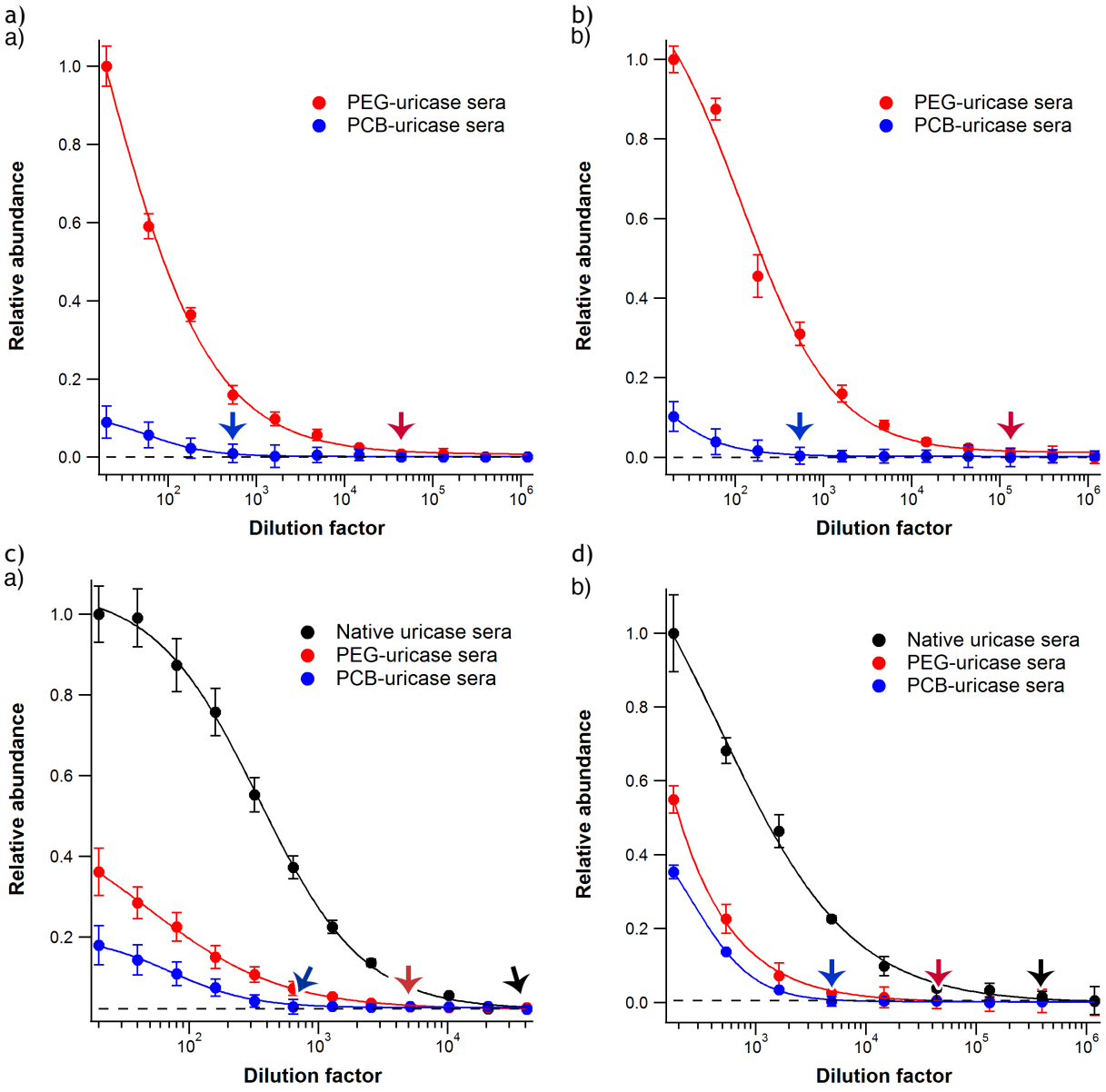

Figure 3-5: Antibody response measured from serum samples collected after multiple injections. IgM (a) and IgG (b) titers were detected using PEG or PCB for their respective polymer-specific antibody content. The same detection was done against uricase for IgM (c) and IgG (d) titers for protein-specific antibody abundance. The arrows denote the antibody titer of each enzyme formulation and the error bars represent standard deviation among assay replicates.

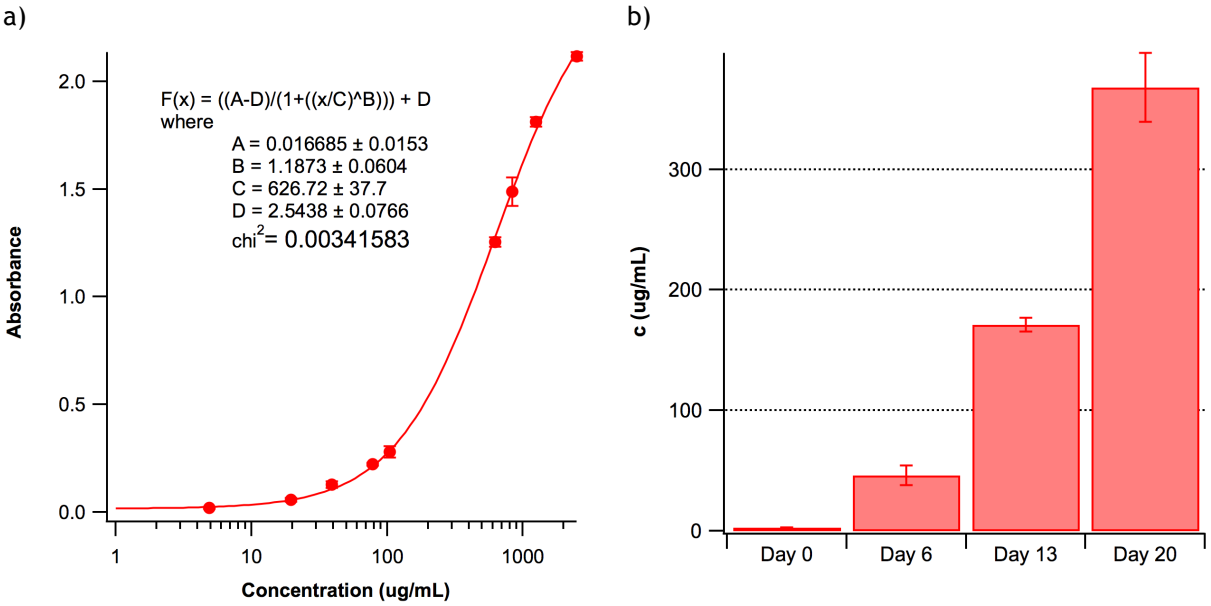

Figure 3-6: Standard curve generated using purified rat anti-PEG IgM (a), which was used in quantifying anti-PEG IgM present in rats that received PEG-uricase (b). The error bar is standard deviation among 4 rats.

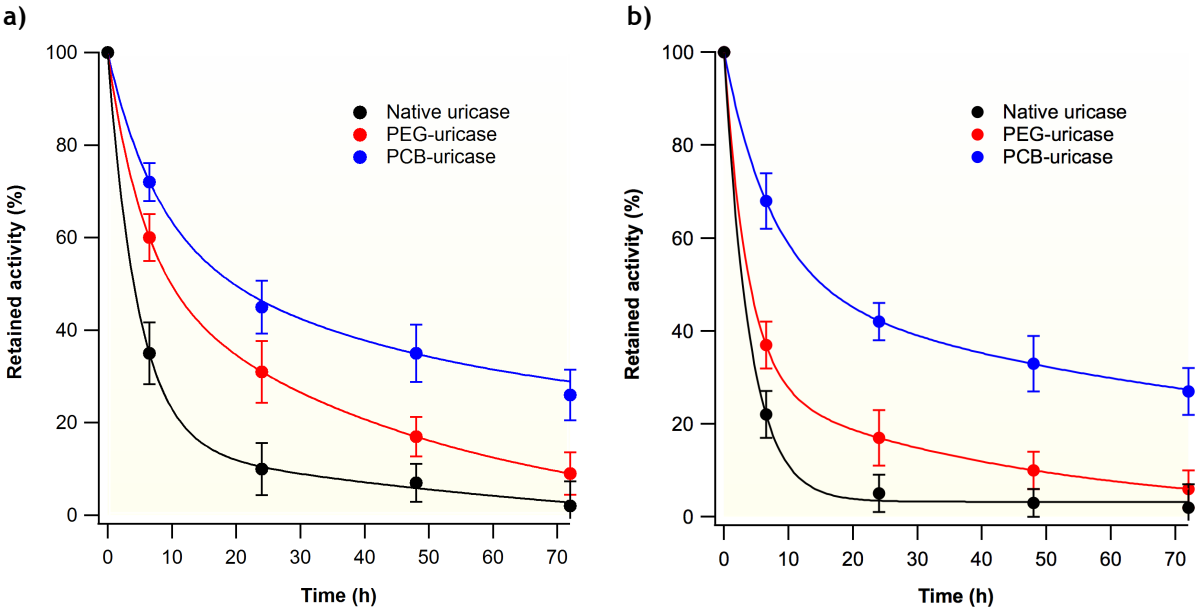

Figure 3-7: Circulation profile of native or polymer-conjugated uricase after (a) one and (b) three repeated weekly injections using residual activity as a surrogate marker. The error bars represent standard deviation among 4 rats.

Table 3-1: Physical parameters of free polymers and native and bioconjugated uricase derived from size-exclusion chromatography and activity measurements.

	MW (kDa)	PDI	#/monomer	Relative activity
Native uricase	140	1.06	--	100%
PEG	10	1.01	6-8	--
PEG-uricase	420±40	1.13	--	95%±5%
PCB	11 (by R_h)	1.19	5-7	--
PCB-uricase	380±44	1.17	--	97%±2%

Table 3-2: ELISA results of serum samples diluted 1:20 in detection buffer.

Serum samples	Relative IgM OD	Stdev	Relative IgG OD	Stdev
Negative control	0.084	0.028	0.087	0.027
Positive control	3.159	0.025	--	--
PEG-uricase	1	0.051	1	0.033
PCB-uricase	0.089	0.041	0.102	0.037

Table 3-3: Pharmacokinetic parameters of uricase and bioconjugates calculated from the two-compartment model.

		First injection		Last injection	
Formulation	**Dosage**	**Elimination half-life (h)**	**Relative bioavailability**	**Elimination half-life (h)**	**Relative bioavailability**
Native uricase	1 mg per kg	13.1 (1x)	1x	6.2 (0.47x)	0.48x
PEG-uricase	1 mg protein per kg rat	37.2 (2.8x)	2.2x	25.6 (2.0x)	1.4x
PCB-uricase	1 mg protein per kg rat	78.4 (6x)	5.4x	78.1 (5.9x)	5.2x

3.7 References

1 Mahmood, I. & Green, M. D. Pharmacokinetic and pharmacodynamic considerations in the development of therapeutic proteins. *Clinical Pharmacokinetics* **44**, 331-347, doi:10.2165/00003088-200544040-00001 (2005).

2 Putney, S. D. & Burke, P. A. Improving protein therapeutics with sustained-release formulations. *Nature Biotechnology* **16**, 153-157, doi:10.1038/nbt0298-153 (1998).

3 Schellekens, H. Bioequivalence and the immunogenicity of biopharmaceuticals. *Nature Reviews Drug Discovery* **1**, 457-462, doi:10.1038/nrd818 (2002).

4 Kolate, A., Baradia, D., Patil, S., Vhora, I., Kore, G. *et al*. PEG - A versatile conjugating ligand for drugs and drug delivery systems. *Journal of Controlled Release* **192**, 67-81, doi:10.1016/j.jconrel.2014.06.046 (2014).

5 Bailon, P., Palleroni, A., Schaffer, C. A., Spence, C. L., Fung, W. J. *et al*. Rational design of a potent, long-lasting form of interferon: A 40 kDa branched polyethylene glycol-conjugated interferon alpha-2a for the treatment of hepatitis C. *Bioconjugate Chemistry* **12**, 195-202, doi:10.1021/bc000082g (2001).

6 Monkarsh, S. P., Ma, Y. M., Aglione, A., Bailon, P., Ciolek, D. *et al*. Positional isomers of monopegylated interferon alpha-2a: Isolation, characterization, and biological activity. *Analytical Biochemistry* **247**, 434-440, doi:10.1006/abio.1997.2128 (1997).

7 Cheng, T. L., Wu, P. Y., Wu, M. F., Chern, J. W. & Roffler, S. R. Accelerated clearance of polyethylene glycol-modified proteins by anti-polyethylene glycol IgM. *Bioconjugate Chemistry* **10**, 520-528, doi:10.1021/bc980143z (1999).

8 Ishida, T., Ichihara, M., Wang, X., Yamamoto, K., Kimura, J. *et al*. Injection of PEGylated liposomes in rats elicits PEG-specific IgM, which is responsible for rapid elimination of a second dose of PEGylated liposomes. *Journal of Controlled Release* **112**, 15-25, doi:10.1016/j.jconrel.2006.01.005 (2006).

9 Ishida, T., Kashima, S. & Kiwada, H. The contribution of phagocytic activity of liver macrophages to the accelerated blood clearance (ABC) phenomenon of PEGylated liposomes in rats. *Journal of Controlled Release* **126**, 162-165, doi:10.1016/j.jconrel.2007.11.009 (2008).

10 Shimizu, T., Ichihara, M., Yoshioka, Y., Ishida, T., Nakagawa, S. *et al*. Intravenous Administration of Polyethylene Glycol-Coated (PEGylated) Proteins and PEGylated Adenovirus Elicits an Anti-PEG Immunoglobulin M Response. *Biological & Pharmaceutical Bulletin* **35**, 1336-1342 (2012).

11 Yang, Q. & Lai, S. K. Anti-PEG immunity: emergence, characteristics, and unaddressed questions. *Wiley Interdisciplinary Reviews-Nanomedicine and Nanobiotechnology* **7**, 655-677, doi:10.1002/wnan.1339 (2015).

12 Armstrong, J. K., Leger, R., Wenby, R. B., Meiselman, H. J., Garratty, G. *et al*. Occurrence of an antibody to poly(ethylene glycol) in normal donors. *Blood* **102**, 556A-556A (2003).

13 Armstrong, J., Hempel, G., Koling, S., Chan, L. S., Meiselman, H. J. *et al*. Rapid clearance of PEG-asparaginase in ALL patients by an antibody against poly (ethylene glycol). *Blood* **108**, 526A-526A (2006).

14 Armstrong, J. K., Hempel, G., Koling, S., Chan, L. S., Fisher, T. *et al*. Antibody against poly(ethylene glycol) adversely affects PEG-asparaginase therapy in acute lymphoblastic leukemia patients. *Cancer* **110**, 103-111, doi:10.1002/cncr.22739 (2007).

15 Cao, Z. Q., Yu, Q. M., Xue, H., Cheng, G. & Jiang, S. Nanoparticles for Drug Delivery Prepared from Amphiphilic PLGA Zwitterionic Block Copolymers with Sharp Contrast in Polarity between Two Blocks. *Angewandte Chemie-International Edition* **49**, 3771-3776, doi:10.1002/anie.200907079 (2010).

16 Cheng, G., Mi, L., Cao, Z. Q., Xue, H., Yu, Q. M. *et al*. Functionalizable and Ultrastable Zwitterionic Nanogels. *Langmuir* **26**, 6883-6886, doi:10.1021/la100664g (2010).

17 Zhang, L., Xue, H., Cao, Z. Q., Keefe, A. J., Wang, J. N. *et al*. Multifunctional and degradable zwitterionic nanogels for targeted delivery, enhanced MR imaging, reduction-sensitive drug release, and renal clearance. *Biomaterials* **32**, 4604-4608, doi:10.1016/j.biomaterials.2011.02.064 (2011).

18 Cao, Z. Q., Zhang, L. & Jiang, S. Superhydrophilic Zwitterionic Polymers Stabilize Liposomes. *Langmuir* **28**, 11625-11632, doi:10.1021/la302433a (2012).
19 Zhang, L., Cao, Z. Q., Li, Y. T., Ella-Menye, J. R., Bai, T. *et al*. Softer Zwitterionic Nanogels for Longer Circulation and Lower Splenic Accumulation. *Acs Nano* **6**, 6681-6686, doi:10.1021/nn301159a (2012).
20 Zhang, L., Xu, J. J., Mi, L., Gong, H., Jiang, S. *et al*. Multifunctional magnetic-plasmonic nanoparticles for fast concentration and sensitive detection of bacteria using SERS. *Biosensors & Bioelectronics* **31**, 130-136, doi:10.1016/j.bios.2011.10.006 (2012).
21 Yang, W., Liu, S., Bai, T., Keefe, A. J., Zhang, L. *et al*. Poly(carboxybetaine) nanomaterials enable long circulation and prevent polymer-specific antibody production. *Nano Today* **9**, 10-16, doi:10.1016/j.nantod.2014.02.004 (2014).
22 Zhang, P., Sun, F., Tsao, C., Liu, S., Jain, P. *et al*. Zwitterionic gel encapsulation promotes protein stability, enhances pharmacokinetics, and reduces immunogenicity. *Proceedings of the National Academy of Sciences* **112**, 12046-12051, doi:10.1073/pnas.1512465112 (2015).
23 Keefe, A. J. & Jiang, S. Poly(zwitterionic)protein conjugates offer increased stability without sacrificing binding affinity or bioactivity. *Nature Chemistry* **4**, 60-64, doi:10.1038/nchem.1213 (2012).
24 Ganson, N. J., Kelly, S. J., Scarlett, E., Sundy, J. S. & Hershfield, M. S. Control of hyperuricemia in subjects with refractory gout, and induction of antibody against poly(ethylene glycol) (PEG), in a phase I trial of subcutaneous PEGylated urate oxidase. *Arthritis Research & Therapy* **8**, doi:10.1186/ar1861 (2006).
25 Sundy, J. S., Ganson, N. J., Kelly, S. J., Scarlett, E. L., Rehrig, C. D. *et al*. Pharmacokinetics and pharmacodynamics of intravenous PEGylated recombinant mammalian urate oxidase in patients with refractory gout. *Arthritis and Rheumatism* **56**, 1021-1028, doi:10.1002/art.22403 (2007).
26 Freitas, D. d. S., Spencer, P. J., Vassao, R. C. & Abrahao-Neto, J. Biochemical and biopharmaceutical properties of PEGylated uricase. *International Journal of Pharmaceutics* **387**, 215-222, doi:10.1016/j.ijpharm.2009.11.034 (2010).
27 Hershfield, M. S., Roberts, L. J., II, Ganson, N. J., Kelly, S. J., Santisteban, I. *et al*. Treating gout with pegloticase, a PEGylated urate oxidase, provides insight into the importance of uric acid as an antioxidant in vivo. *Proceedings of the National Academy of Sciences of the United States of America* **107**, 14351-14356, doi:10.1073/pnas.1001072107 (2010).

CHAPTER 4

EFFECT OF POLYMER LENGTH AND DENSITY ON ENZYME PROTECTION FROM HUMORAL RESPONSE

Sijun Liu, Zhefan Yuan, and Shaoyi Jiang

Abstract

Previously, we studied the protection of an immunogenic protein, uricase, by conjugating either the zwitterionic polymer poly(carboxybetaine) or the non-ionic polymer poly(ethylene glycol). In order to maintain applicable comparisons, we utilized both polymer of the same hydrodynamic size. In this work, we want to examine whether adjusting the ratio between length of the zwitterionic polymer and degree of protein conjugation would minimize immune recognition further. To that end, we synthesized polymers with 10 kDa, 20 kDa, and 30 kDa molecular weights, prepared protein conjugates that maximized polymer density for each size, and studied their effect in vivo on the humoral response elicited against the underlying immunogenic protein. We hypothesize that the smaller polymers would conjugate in higher density, adopting a brush-like confirmation, while the longer polymers may be sparse but may extend each chain over a larger surface area. Taking into consideration circulation profile and antibody generation, we found the 10-kDa polymer may be too short and the 30-kDa polymer too few in number to shield effectively; the 20-kDa polymer remain the best choice in terms of balancing conjugation density and epitope coverage.

4.1 Introduction

As poly(ethylene glycol) (PEG) is the leading polymer for bioconjugation and biomaterial modification, it is the most widely studied polymer in terms of immunogenicity. Up until recently, PEG was lauded as a non-immunogenic protein, as it conferred stealth characteristics to problematic therapeutics by providing a steric protective polymer shell. However, studies in the clinic and academia have since debunked its assumed innocuousness. Out of the twelve FDA-approved PEGylated therapeutics, two (pegasparaginase and pegloticase) resulted in a loss of efficacy due to the presence of anti-drug (and anti-polymer) antibodies.[1,2] Anti-PEG antibodies were also detected in healthy blood donors or patients who never received PEGylated therapeutics, alerting to the presence of pre-existing anti-PEG antibodies.[3,4] This is possibly due to the excess exposure of PEG or PEG-like molecules (e.g. Tween) in industrial formulations, consumer products, or cosmetics.

Antibody generation towards biomaterials and therapeutics is a complicated process, often mediated by several factors. In the case of PEG, early studies showed that the immunogenicity of the carrier protein affects the antibody response toward the polymer itself, much like the way haptens becomes immunogenic due to attachment to the larger proteins.[5] This is corroborated by work utilizing bovine serum albumin[6], which is a highly conserved protein and thus tolerated by mammalian host immune systems. This work also demonstrated that increasing density of grafted polymers decreases the antibody response, where the more robust shell serves to better shield antigenic epitopes from recognition. More recent studies attributed the immunogenicity to the chemical nature of PEG, where its hydrophobic backbone and end groups were sites of recognition for the anti-PEG antibodies generated.[7,8]

In our previous work[9], we demonstrated our zwitterionic polymer PCB can improve the shortcomings of PEG in terms of anti-protein and anti-polymer antibody reduction. In this work, we are interested in studying the effects of PCB conjugation in detail in order to ascertain a combination of polymer length and grafting density that may result in minimal anti-protein antibody production while maintain longer circulation properties. Unlike PEG, the completely hydrophilic nature of PCB also confers an advantage. We hypothesize that among the therapeutically relevant sizes of 10, 20, and 30 kDa molecular weight (MW), the smaller the polymer the higher the grafting density, but the polymer

may not be long enough to provide great shielding of epitopes; the longer polymer shell will be sparser, but it may be the right combination of polymer length to density for ideal coverage.

4.2 Materials and methods

4.2.1 Materials

All chemicals (unless otherwise specified), recombinant uricase from *Candida sp*. expressed in *E. coli* (U0880-1000UN), and xanthine agarose (X3128-1ML) for affinity chromatography were purchased from Sigma-Aldrich (St. Louis, MO). Amplex Red Uricase Assay kits (A22181), Costar 96-well EIA/RIA plates (07-200-721), and the 3,3',5,5'-Tetramethylbenzidine (TMB) substrate solution (34028) were purchased from Thermo Fisher Scientific (Waltham, MA). Female Sprague Dawley rats (SAS SD, strain code 400) of 101-125 g were purchased from Charles River Laboratories (Burlington, MA). Sterile 0.22 μm Millex-GP syringe filters (SLGV004SL) and Amicon Ultra centrifugal filter units (UFC510096) were purchased from EMD Millipore (Billerica, MA). Goat anti-rat antibodies (ab97057 and ab97180) were purchased from Abcam (Massachusetts, US).

4.2.2 Synthesis of PCB polymers of differing lengths

PCB polymers of 10-, 20-, and 30-kDa absolute molecular weight were synthesized as previously described in Section 2.2.3 via reversible addition-fragmentation chain-transfer polymerization. The monomer to chain transfer agent (CTA) molar ratio was 40:1, 70:1, and 120:1, respectively, and the initiator AIBN to CTA ratio was kept at 0.2:1 for all three. Reaction time was 4 h for the smaller polymers and 6 h for the largest polymer. The CTA was then cleaved using hexylamine, revealing a thiol group capable of bioconjugation.

4.2.3 Preparation of uricase-PCB conjugates

Uricase conjugates were prepared by first reacting the protein to the heterobifunctional NHS-maleimide crosslinker AMAS at 2 eq total lysine in phosphate-buffered saline (PBS), pH 7.4, for 1 h at RT. Any unreacted crosslinker was removed via multiple rounds of spin dialysis. Then, SH-terminated PCB polymer was added at 40 eq in 0.1M borate buffer, pH 8.5, for 2 h at RT. Again the unreacted

excess polymer was removed via multiple rounds of spin dialysis, using PBS as the eluting buffer. Protein solutions were stored at 4 °C until use.

4.2.4 Protein conjugate analysis via size-exclusion chromatography

All samples were processed in a 1260 Infinity binary high performance liquid chromatography (HPLC) system equipped with a UV detector (Agilent Technologies, Santa Clara, CA), a miniDAWN TREOS light scattering (LS) detector, and a Optilab T-rEX differential refractive index (dRI) detector (Wyatt Technology, Santa Barbara, CA). The flow rate was set at 0.6 mL/min with the mobile phase PBS (pH 7.4) with 0.02% sodium azide as a preservative. The Waters Ultrahydrogel 1000 column (7.8 mm x 300 mm, 12 μm particle size) was used for fractionating polymer-protein conjugates. The degree of polymer conjugation for each conjugate was calculated using the dn/dc values of the protein and polymer and the "Protein Conjugate" method supplied by the ASTRA software.

4.2.5 Animal studies

The University of Washington Institutional Animal Care and Use Committee reviewed and approved all animal experiments under protocol #4203-01 prior to conducting studies. Female Sprague Dawley rats of ~150 g were randomly divided into groups of three, one group each for bare enzyme, uricase-PCB_{10k}, uricase-PCB_{20k}, and uricase-PCB_{30k} conjugates. Weights were recorded at days 0, 7, and 14 to ascertain the volume of administration for formulations of 1 mg protein/mL PBS to be administered at 1 mg uricase per kg animal (**Figure 4-1**). Also on day 0, baseline sera were generated from blood collected from each animal. On days 1, 8, and 15, each enzyme formulation was administered into the rat tail vein under aseptic surgical conditions with isoflurane anesthesia. On days 15-18, blood was sampled ~5 min, 4 h, 10 h, 24 h, 48 h, and 72 h post injection to generate a circulation profile of the different protein formulations as affected by possible antibody production. On days 25 and 36, blood was sampled for IgM and IgG detection, respectively, and the animals were euthanized after final blood collection. All blood samples were treated by allowing clotting to occur at room temperature for approximately 30 min, centrifuged to pellet the cellular debris, and the clear supernatant was collected as serum samples and frozen in small aliquots until use.

4.2.6 Enzyme-specific antibody detection

Indirect enzyme-linked immunosorbent assay (ELISA) experimental conditions previously developed were used to detect uricase-specific antibodies. Native uricase was adsorbed onto the plate in in 100 µL/well carbonate/bicarbonate buffer (0.2 M, pH 9.4) at 1 µg enzyme/well for over night at 4 °C. After 2x wash using PBS supplemented with 0. 5% (w/v) Tween-20, the plate was blocked with 5% nonfat dry milk solution at RT for 2 h. After another 2x wash, pooled serum samples (in order to conserve the small volumes we obtained due to bleed volume constraints by the IACUC guidelines) along with controls are added in duplicate and incubated for 2 h at RT followed by 5x wash. Detection antibody (goat anti-rat IgM IgG or goat anti-rat IgG IgG) diluted 1:20,000 is then added and incubated at RT for 1 h. After 5x wash, the TMB substrate solution was added for 15 min and quenched with 2 N H_2SO_4 stop solution. The plates were measured for absorbance at 450 nm with 570 nm values as background subtraction. Native uricase serum samples were used as positive control and pre-experiment blood samples were used as negative control.

4.2.7 Determination of circulation profile

The Amplex Red Uricase Assay kits were used following manufacturer's instructions to ascertain specific activity of bare uricase and the uricase conjugates as a surrogate marker for blood concentration. The circulation plots were generated and the IgorPro software was used to calculate the elimination half-life (ln 2/ß) and relative bioactivity (integral of circulation curve from zero to infinity) of each formulation by fitting the data to a two-phase exponential decay function that describes two-component pharmacokinetics, $C(t) = a \cdot e^{-\alpha t} + b \cdot e^{-\beta t}$.

4.3 Results and discussions

4.3.1 Bioconjugation with PCB polymers of various lengths

Polymer conjugation onto protein surfaces via nonspecific amine chemistry is largely governed by solvent accessibility to the ε-amino end groups on lysines. As polymers are relatively bulky macromolecules, the attachment of one strand may hinder a neighboring lysine from further

conjugation. We synthesized three different lengths of PCB polymers, 10 kDa, 20 kDa, and 30 kDa, to examine if length will significantly affect grafting density and enzyme protection. We hypothesized that the shortest PCB polymer should achieve the highest loading density, but may fail to protect all the immunogenic epitopes.

Zwitterionic polymers are smaller in hydrodynamic size (R_H) than their absolutely molecular weight (MW) would suggest, much like a globular protein. Figure 4-2a shows the chromatography profile of the three polymers, where they elute with nonionic polymer standards of about half their absolute MW. We then conjugated each length of polymer onto the model enzyme uricase, and interestingly all three conjugates yielded approximately the same R_H MW via SEC (Figure 4-2b, Table 4-1). We believe this is due to the aforementioned steric hindrance, where only so many polymers may be grafted in proximity, depending on the length each chain.

4.3.2 Protection from protein-specific humoral response

In previous work[9], we demonstrated a decrease in but not elimination of uricase-specific IgM and IgG post PCB conjugation. In this work, we hoped to observe a difference due to the differing polymer conformation afforded by the varying lengths. In Figure 4-3, the IgM dilution titer is about 1/1,600 for all three PCB-conjugated uricase, which is about a 64-fold improvement upon the native uricase (1/102,400 dilution titer). The relative difference between the protein conjugates are more obvious in the IgG dilution titers, where the 20-kDa conjugate had the lowest titer at 1/1,600 while the 10-kDa increased to 1/6,400 and the 30-kDa to 1/12,800. All three are still vastly superior to the native uricase, which was still detected at 1/102,400. This translates to a 64-fold, 16-fold, and 8-fold improvement for 10-kDa, 20-kDa, and 30-kDa conjugates, respectively.

4.3.3 The effect of circulating antibodies on conjugate circulation

Upon repeated exposure to the same antigen, the immune system becomes more and more efficient at mounting a response and thus resulting in faster clearance of the foreign agent. In this study, the circulation profile of the third injection of native and PCB-conjugated uricase is summarized in Figure 4-4. Even though 20-kDa polymer-uricase conjugates performed the best via antibody

reduction, the 10-kDa PCB-uricase conjugate had the longest circulation residence time. We believe this might be due to the time difference between the circulation and antibody blood collections: if we had studied the circulation of a fourth injection, we would likely discover that the 20-kDa polymer-protein conjugate is now the longest circulating.

4.4 Conclusions

As we expected, increasing the MW of the polymer adversely affected the grafting density of the resultant protein conjugate. Out of the three lengths of polymers studied, 10, 20, or 30 kDa, the middle length yielded the least anti-protein antibody while maintaining long circulation. These results cemented our selection of using the 20-kDa polymer for future studies. Interesting, this size correlates to the 10-kDa PEG, which is the most popular MW for therapeutic use. Perhaps this length remains the most ideal between grafting density and epitope coverage.

4.5 Acknowledgments

We gratefully acknowledge the funding agencies for supporting this work: National Institutes of Health (1R21EB020781-01) and Defense Threat Reduction Agency (HDTRA1-13-1-0044).

4.6 Figures, schemes, and tables

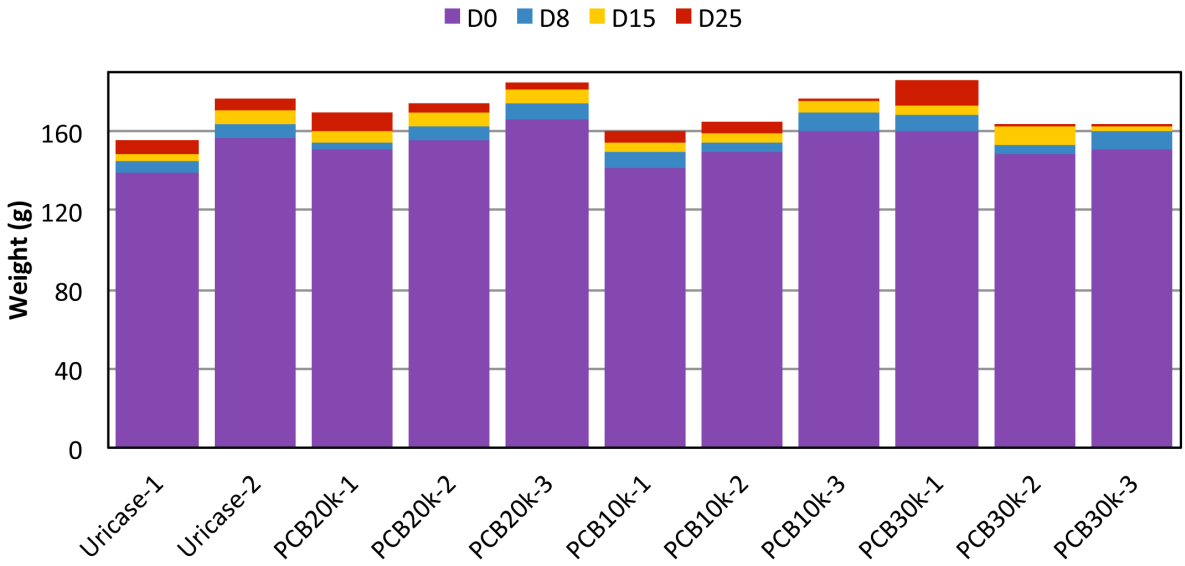

Figure 4-1: Animal weight record over the study period.

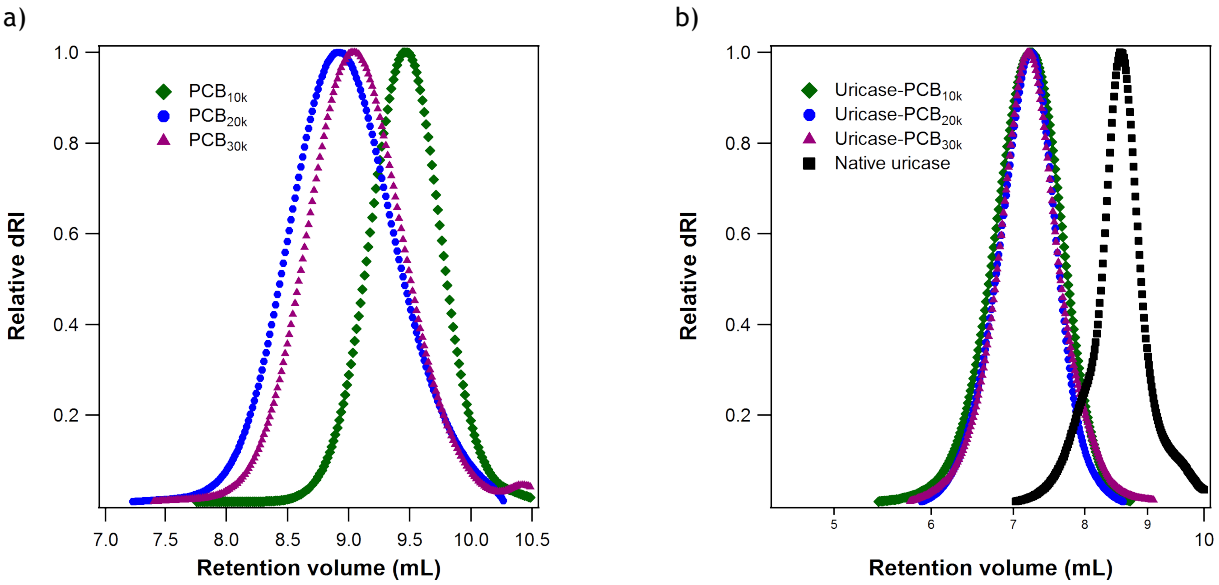

Figure 4-2: Size-exclusion chromatogram of polymers alone (a) and conjugated (b) to uricase.

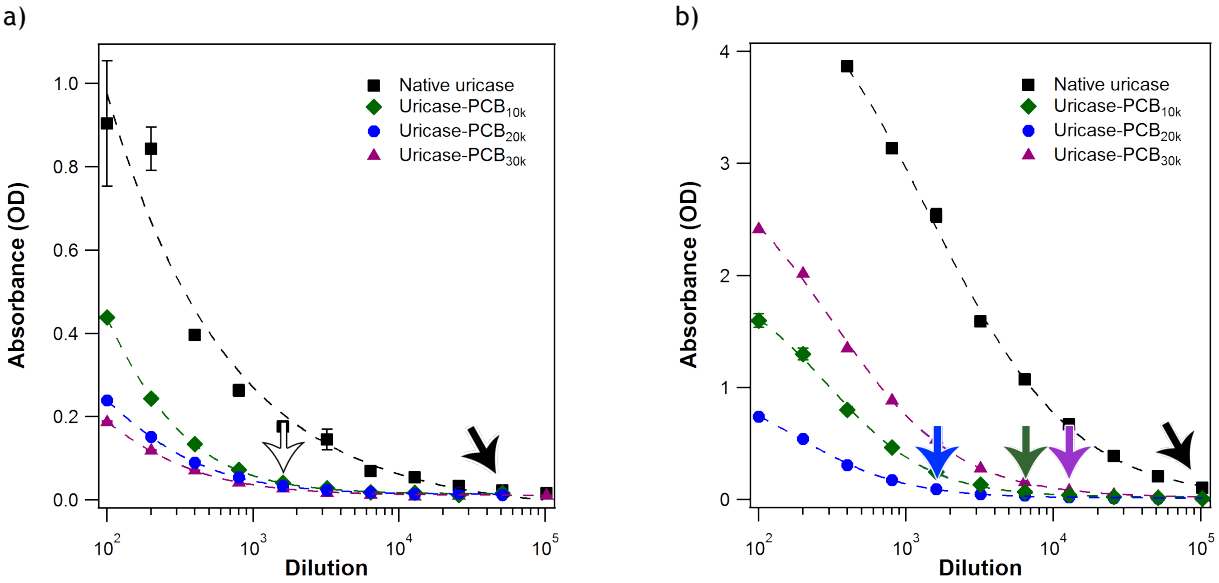

Figure 4-3: Antibody dilution profile of (a) IgM and (b) IgG elicited against native and various polymer-conjugated uricase. The error bars represent standard deviation.

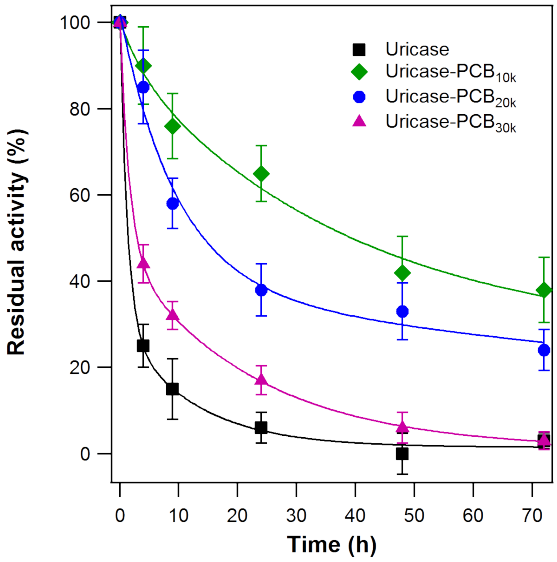

Figure 4-4: Circulation profiles of native and PCB-modified uricase conjugates after three injections, using pooled blood from three animals. The fit curves were calculated using two-component exponential decay via the least-squares method.

Table 4-1: Physical parameters of PCB polymers and PCB-uricase conjugates.

	MW (kDa)	PDI	#/monomer
Native uricase	140	1.056	--
PCB_{10k}	9.5	1.04	--
PCB_{10k}-uricase			7-8
PCB_{20k}	19.7	1.113	--
PCB_{20k}-uricase			5-6
PCB_{30k}	32.1	1.144	--
PCB_{30k}-uricase			2-3

Table 4-2: Pharmacokinetic parameters of the native and uricase conjugates.

Formulation	Dosage	Elimination half-life (h)	Relative bioavailability
Native uricase	1 mg per kg	6.9 (1x)	1x
PCB_{10k}-uricase	1 mg protein per kg rat	86 (12.5x)	12x
PCB_{20k}-uricase	1 mg protein per kg rat	75 (10.9x)	7.9x
PCB_{30k}-uricase	1 mg protein per kg rat	11 (1.6x)	1.6x

4.7 References

1 Armstrong, J., Hempel, G., Koling, S., Chan, L. S., Meiselman, H. J. *et al*. Rapid clearance of PEG-asparaginase in ALL patients by an antibody against poly (ethylene glycol). *Blood* **108**, 526A-526A (2006).

2 Hershfield, M. S., Ganson, N. J., Kelly, S. J., Scarlett, E. L., Jaggers, D. A. *et al*. Induced and pre-existing anti-polyethylene glycol antibody in a trial of every 3-week dosing of pegloticase for refractory gout, including in organ transplant recipients. *Arthritis Research & Therapy* **16**, doi:10.1186/ar4500 (2014).

3 Armstrong, J. K., Leger, R., Wenby, R. B., Meiselman, H. J., Garratty, G. *et al*. Occurrence of an antibody to poly(ethylene glycol) in normal donors. *Blood* **102**, 556A-556A (2003).

4 Richter, A. W. & Akerblom, E. Polyethylene-glycol reactive antibodies in man - titer distribution in allergic patients treated with monomethoxy polyethylene-glycol modified allergens or placebo, and in healthy blood-donors. *International Archives of Allergy and Applied Immunology* **74**, 36-39 (1984).

5 Richter, A. W. & Akerblom, E. Antibodies against polyethylene-glycol produced in animals by immunization with monomethoxy polyethylene-glycol modified proteins. *International Archives of Allergy and Applied Immunology* **70**, 124-131 (1983).

6 Abuchowski, A., Vanes, T., Palczuk, N. C. & Davis, F. F. Alteration of immunological properties of bovine serum-albumin by covalent attachment of polyethylene-glycol *Journal of Biological Chemistry* **252**, 3578-3581 (1977).

7 Sherman, M. R., Williams, L. D., Sobczyk, M. A., Michaels, S. J. & Saifer, M. G. P. Role of the Methoxy Group in Immune Responses to mPEG-Protein Conjugates. *Bioconjugate Chemistry* **23**, 485-499, doi:10.1021/bc200551b (2012).

8 Saifer, M. G. P., Williams, L. D., Sobczyk, M. A., Michaels, S. J. & Sherman, M. R. Selectivity of binding of PEGs and PEG-like oligomers to anti-PEG antibodies induced by methoxyPEG-proteins. *Molecular Immunology* **57**, 236-246, doi:10.1016/j.molimm.2013.07.014 (2014).

9 Liu, S. & Jiang, S. Zwitterionic polymer-protein conjugates reduce polymer-specific antibody response. *Nano Today* **11**, 285-291 (2016).

CHAPTER 5

PROTECTION OF ORGANOPHOSPHATE-NEUTRALIZING ENZYMES

Sijun Liu, Zhefan Yuan, Erik Liu, and Shaoyi Jiang

Abstract

Organophosphates (OP) agents are chemical weapons of mass destruction, which act through the inactivation of acetylcholinesterase, leading to detrimental effects such as muscular paralysis, convulsions, bronchial constrictions, and death by asphyxiation. The common detoxification strategies include the scavenger protein butyrylcholinesterase (BChE) and the OP-degrading enzyme organophosphorus hydrolase (OPH). Shortcomings of these methods are two-fold: first, the enzyme needs to maintain long circulation times as preventative prophylaxis, and secondly, its bacterial source and recombinant production will have immunogenic consequences that lower therapeutic effect. Zwitterionic materials can solve both of these problems and may improve the binding affinity and bioactivity of the enzyme. Building on these encouraging past results, we augmented detoxification enzymes by grafting PCB polymers to the protein surfaces. By using both the full-spectrum OP-sequestering BChE and OP-neutralizing OPH, we investigated the effect of polymer conjugation on (i) normal enzymatic functions (activity), (ii) circulation and residence time in vivo, and (iii) acute inflammation and antibody response toward the exogenous OPH. We found the PCB polymer conjugation did not hinder enzyme activity, improved the circulation profile and in vivo residence time, and alleviated polymer-specific antibody responses.

5.1 Introduction

Organophosphates (OPs) are small molecules utilized as pesticides, but also exploited as chemical weapons of mass destruction. They act through the irreversible inactivation of acetylcholinesterase (AChE), an enzyme that degrades the neurotransmitter acetylcholine (ACh) and is essential to the normal functioning of nerve cells. OPs mimic ACh by substituting a phosphate for the acetate group, allowing them to be recognized by the AChE active site. However, once the leaving group dissociates after hydrolysis, the phosphorylated enzyme cannot regenerate the free active site as normal (Error! Reference source not found.) and ceases to modulate ACh levels.[1] Excess ACh results in impeded neurotransmission, leading to detrimental effects such as muscular paralysis, convulsions, bronchial constrictions, and death by asphyxiation.[2]

One of two common detoxification strategies is the enzyme butyrylcholinesterase (BChE).[3,4] As the name suggests, BChE is a naturally occurring human hydrolase of cholines and its active site is capable of binding OP compounds. While AChE is present mostly in organs like the brain and muscles (neuromuscular junctions), BChE has significantly more activity in plasma: 3,300 ng BChE/mL versus 8 ng/mL of AChE/mL.[5] This means BChE can neutralize OP in circulation prior to AChE inactivation at synaptic junctions. As such, it functions as a stoichiometric biological scavenger and requires high doses to achieve the desired therapeutic effect.[6] The larges-scale production of this human enzyme has been challenging and the supply issue is hindering progress toward clinical trials.[7] Despite these shortcomings, it is currently the only prophylactic agent under consideration by the Food and Drug Administration that provides protection against the full spectrum of neurotoxins.[8]

Another method of neutralization utilizes microbial enzymes capable of degrading the nerve agents.[3] Organophosphorus hydrolase (OPH) has the widest range of substrate specificity and thus extensively investigated for therapeutic use. As a phosphotriesterase, OPH can hydrolyze P—O, P—F, P—S, and P—C bonds[1] and is thus effective against G-type (sarin/GB, cyclosarin/GF, and soman/GD) and V-type (VX and VR) OPs[9] (Scheme 5-2). For an average-sized human, VX is around 200 times more toxic than soman and 300 times more than sarin[10], but unfortunately wildtype OPH is about 1,000 times more active toward G-type agents[9]. The United States government has supported considerable efforts

exerted toward generating more V type-selective OPH variants, but studies are limited to the in vitro activity measurements at this time.

Shortcomings of enzymatic remedial methods of OP agents are two-fold: first, the enzyme needs to maintain long circulation times as preventative prophylaxis, and secondly, its bacterial source and/or recombinant production will have immunogenic consequences that lower residence time and thus therapeutic effect. Zwitterionic materials can solve both of these problems, as multiple studies demonstrated their ability to confer long circulation times and evasion from detection of the immune system.[11-13] Furthermore, evidence suggested that conjugation of the zwitterionic poly(carboxybetaine) polymer (PCB) can improve the binding affinity and substrate activity of the enzyme.[14] Building on these encouraging past results, we propose to augment detoxification enzymes by grafting PCB polymers to the protein surfaces. By using both the OP-neutralizing OPH, we will investigate the effect of polymer conjugation on (i) normal enzymatic functions (activity), (ii) circulation profile and residence time in vivo, and (iii) acute inflammatory responses to as well as antibody production against the exogenous OPH.

5.2 Materials and methods

5.2.1 Materials

All chemicals were purchased from Sigma-Aldrich (St. Louis, MO). Antibodies were purchased from Abcam (Massachusetts, US). Costar 96-well EIA/RIA plates, Pierce BCA Protein Assay Kit, 3,3',5,5'-Tetramethylbenzidine (TMB) substrate solution, and Amicon Protein Concentrators (10 kDa and 50 kDa MWCO) were purchased from Thermo Fisher Scientific (Waltham, MA). The IL-1b and TNF-α cytokine kits were purchased from eBioscience (San Diego, CA). The IL-6 cytokine kit was purchased from BD Biosciences (Franklin Lakes, NJ).

5.2.2 Expression of OPH

A gene encoding for OPH was inserted into a pET-20b(+) vector (kindly gifted by Dr. Andrew Bigley) between the NdeI and EcoRI restriction sites as previously described[9]. The expression vector was transformed into *E. coli* BL21(de3) cells. Transformants were cultured in 5 mL Terrific Broth (TB)

supplemented with ampicillin for 8 h at 37 °C. 1mL of the culture was used to inoculate 1L TB supplemented with ampicillin and was grown for 16 hours at 30 °C. The expression culture was then supplemented with 1mM $CoCl_2$ (Fisher Scientific) and induced with 1mM isopropyl ß-D-1-thiogalactopyranoside and allowed to express for 24 h at 30 °C. The culture underwent centrifugation and the cell pellet was resuspended in 100 mL purification buffer (50mM HEPES, 100 µM $CoCl_2$, pH 8.5). The suspension underwent three freeze-thaw cycles and the lysate underwent probe sonication until the lysate was clarified. The lysate underwent centrifugation to remove cellular debris. Then, 4 g protamine sulfate dissolved in 20 mL purification buffer was added to the supernatant and incubated for 20 min before the precipitate was removed through centrifugation. The supernatant was brought to 60% ammonium sulfate saturation and mixed for 30 min before undergoing centrifugation. The pellet was dissolved in up to 5 mL purification buffer and sterile filtered. Further purification was performed on a NGC Quest 10 Chromatography System from Bio-Rad (Hercules, CA). The protein solution first underwent size-exclusion chromatography utilizing the purification buffer on a HiLoad 16/600 Superdex 200 pg column from GE Healthcare Bio-Sciences (Pittsburgh, PA) before undergoing ion exchange chromatography utilizing the purification buffer with an increasing NaCl gradient on an ENrich Q column from Bio-Rad (Hercules, CA).

5.2.3 Preparation of OPH-PCB conjugates

OPH was exchanged from HEPES buffer (pH 8.0) into PBS (pH 7.4) using a 10-kDa MWCO spin column (both buffers were supplemented with 0.1 mM $CoCl_2$). The final concentration was adjusted to 2 mg/mL. The heterobifunctional crosslinker AMAS was dissolved in DMSO and added at 2 eq available lysine. After 1 h reaction at RT, unreacted crosslinkers were removed using multiple rounds of spin dialysis, with the protein solution concentrated to ~2 mg/mL final concentration as determined by protein assay. Then, NHS ester-activated PCB polymers (20 kDa M_n MW) were dissolved to ~10 mg/mL and was combined with the protein solution at ~50 eq by weight. The reaction mixture was gently rocked for 1 h and unreacted polymers were removed by spin dialysis with 50-kDa MWCO spin column. Protein concentration quantifications used a Pierce 660 nm Protein Assay kit, following the instructions of the manufacturer and using bovine serum albumin as a known standard.

5.2.4 *Activity measurement of OPH and OPH-PCB conjugates*

OPH activity was measured by monitoring the change in absorbance at 400 nm in the presence of the substrate paraoxon in 0.1 M sodium phosphate buffer (pH 7.4) supplemented with 0.1 mM $CoCl_2$. The native activity was assessed at a variety of enzyme and paraoxon concentrations to yield parameters suitable to compare with conjugated enzymes. The hydrolysis product *p*-nitrophenol was reconstituted in a range of known concentrations to calculate the extinction coefficient at 400 nm, which is used to convert the kinetic results into concentration units. The graphing software Igor Pro was used to generate fit curves based on Michaelis-Menten, Lineweaver-Burk, and linear equations.

5.2.5 *OPH animal studies for circulation and protein-specific antibody production*

The University of Washington Institutional Animal Care and Use Committee reviewed and approved all animal experiments under protocol #4203-03 prior to conducting studies. Female Sprague Dawley rats of ~150 g were randomly divided into groups of three, one group each for bare enzyme and OPH-PCB_{20k} conjugates. Weights were recorded at days 0, 7, and 14 to ascertain the volume of administration for formulations of 1 mg protein/mL PBS to be administered at 1 mg OPH per kg animal. Also on day 0, baseline sera were generated from blood collected from each animal. On days 1, 8, and 15, each enzyme formulation was administered into the rat tail vein under aseptic surgical conditions with isoflurane anesthesia. On days 1-3 and 15-18, blood was sampled ~5 min, 1 h, 6 h, 11 h, 24 h, 48 h, and 72 h post injection to generate a circulation profile. On days 25 and 36, blood was sampled for IgM and IgG detection, respectively, and the animals were euthanized after final blood collection. All blood samples were treated by allowing clotting to occur at room temperature for approximately 30 min, centrifuged to pellet the cellular debris, and the clear supernatant was collected as serum samples and frozen in small aliquots until use.

5.2.6 *OPH animal studies for acute inflammation via cytokine detection*

The University of Washington Institutional Animal Care and Use Committee reviewed and approved all animal experiments under protocol #4203-03 prior to conducting studies. Female Sprague

Dawley rats of ~150 g were randomly divided into groups of three, one group each for PBS control, bare enzyme, and OPH-PCB_{20k} conjugates. Weights were recorded at days 0 to ascertain the volume of administration for formulations of 1 mg protein/mL PBS to be administered at 1 mg OPH per kg animal. Also on day 0, baseline sera were generated from blood collected from each animal. On days 1, 3, and 5, each sample was administered into the rat tail vein under aseptic surgical conditions with isoflurane anesthesia. Following each injection, blood was sampled at 4 h, 8 h, and 12 h to generate serum for cytokine quantification and the animals were euthanized following the last blood draw. All blood samples were treated by allowing clotting to occur at room temperature for approximately 30 min, centrifuged to pellet the cellular debris, and the clear supernatant was collected as serum samples and frozen in small aliquots until use.

5.3 Results and discussion

5.3.1 Effect of PCB conjugation on OPH activity

OPH follows Michaelis-Menten kinetics and prefers basic environments[9]; however, because it is intended to work in the body, we decided to assay activity at physiological pH. **Figure 5-1a** shows kinetic traces of paraoxon hydrolysis by OPH at different initial concentrations by following the increase in the product *p*-nitrophenol. As hydrolysis reactions are efficient, we assumed paraoxon degradation went to completion and used the final absorbance values to calculate the extinction coefficient of *p*-nitrophenol in our buffer system to convert absorbance values into concentration (Figure 5-1**b)**. Then, the initial linear slope of each trace is calculated and plotted against substrate concentration in **Figure 5-2**, where two different equations are used to estimate the kinetic parameters: the Michaelis constant K_M, the turnover number k_{cat}, and catalytic efficiency k_{cat}/K_M (**Table 5-1**).

After establishing the assay conditions, we selected a unique condition to assess all future activity measurements. For practicality, instead of running the full Michaelis-Menten investigation, we will instead study specific activity, i.e. at a single enzyme and substrate concentration. The side-by-side comparison of native and PCB-modified OPH will yield relative activity. For the PCB-OPH conjugates studied, the relative activity was 92 $\pm$ 3% of the native OPH.

5.3.2 OPH-specific antibody response with or without PCB conjugation

The expression system for OPH is *E. coli*, which suggest that the protein will carry immunogenic epitopes inconveniently ready for immune recognition. This was confirmed by previous animal studies utilizing OPH, which demonstrated the presence of OPH-specific IgG.[15] In this work, we found that the dilution titer of anti-OPH IgM to be 32-fold less in PCB-OPH animals than the native (1/6400 vs. 1/204800, respectively). Anti-OPH IgG titer detected in sera from PCB-OPH animals was 1/6400, compared to 1/102400 detected in the native OPH sera, which correlates to a 16-fold decrease. Both dilution profiles are presented in Figure 5-4. As with previous cases of PCB conjugation, the presence of the superhydrophilic polymer shell greatly decreased immune recognition and resulted in a decline in production of protein-specific antibodies.

5.3.3 Pharmacokinetic properties of native and PCB-conjugated OPH

Compared to the human-sourced OP bioscavenger BChE, the circulation of OPH is much shorter, usually around half an hour in circulation half-life.[1,15] We compared the circulation profiles of both native and PCB-conjugated OPH after multiple injections, in order to observe any change due to accelerated clearance mediated by anti-protein antibodies. As seen in Figure 5-3, there is no significant difference between the first and third injections for both formulations. The half-life of OPH decreased from 0.5 h to 0.3 h and from 9.2 h to 8.7 h for PCB-OPH conjugates (Table 5-2), which translates to about a 18x extension. Due to the inherent different in animal blood volume and weight, these numbers are not significant from each other. Even though we expected a change in clearance due to the presence of anti-protein antibodies, we did not observe it under the current study conditions. We think this is likely due to the existing short circulation for OPH and the limitation of methodology.

5.3.4 Dose tolerance and acute inflammation

As the OPH technology has not been studied in humans, preclinical investigations are important for its development toward meaningful applications. In addition to the routine pharmacokinetic studies

detailed above, we also conducted preliminary examinations in terms of acute inflammation against repeated dosing of the foreign OPH. To this end, we utilized detection of cytokines, which are mediators of immune response. In a pro-inflammatory setting, several key cytokines are released and are signals for the activation and proliferation of certain leukocytes. Depending on the cytokines released, T_{H1} or T_{H2} responses may occur. The first encourages cell-mediated killing, while the latter promotes helper functions that result in the humoral response by B cells. The cytokines we chose to investigate are IL-1b, IL-6, and TNF-α, all notable proinflammatory cytokines produced by activated macrophages. As shown in Figure 5-5, Figure 5-6, and Figure 5-7, there is little presence of any of the three cytokine above control levels, after three injections of a total of ~0.6-0.75 mg/animal. This is an encouraging response, which suggests that up to 3 dosing in relative rapid succession will not result in any acute inflammatory response. However, many more factors still remain to be investigated to better understand the tolerance of OPH for human applications.

5.4 Conclusions and future outlook

We investigated native and PCB-conjugated OPH to compare the benefits afforded by the zwitterionic polymer shell. Our findings suggest that PCB-conjugation can increase circulation residence time while decreasing antibody responses toward the protein. Preliminary studies show that administration of up to three doses within five days will not result in the acute inflammatory response, as measured by relevant cytokines. To examine the dosage tolerance further, we will study cytokine production by immune cells isolated from the spleen and thymus, as well as increasing the dosage from 1 mg/kg to 5 mg/kg and 10 mg/kg. Information from these proposed studies, combined with data already collected, will inform future formulations of OPH for practical use in the field.

5.5 Acknowledgments

We would like to thank the Defense Threat Reduction Agency for funding this work under grant HDTRA1-13-1-0044. We are also grateful of Dr. Douglas Cerasoli (USAMRICD) and Dr. Andrew Bigley (Texas A&M University) for valuable discussions regarding OPH expression and characterization.

5.6 Schemes, figures and tables

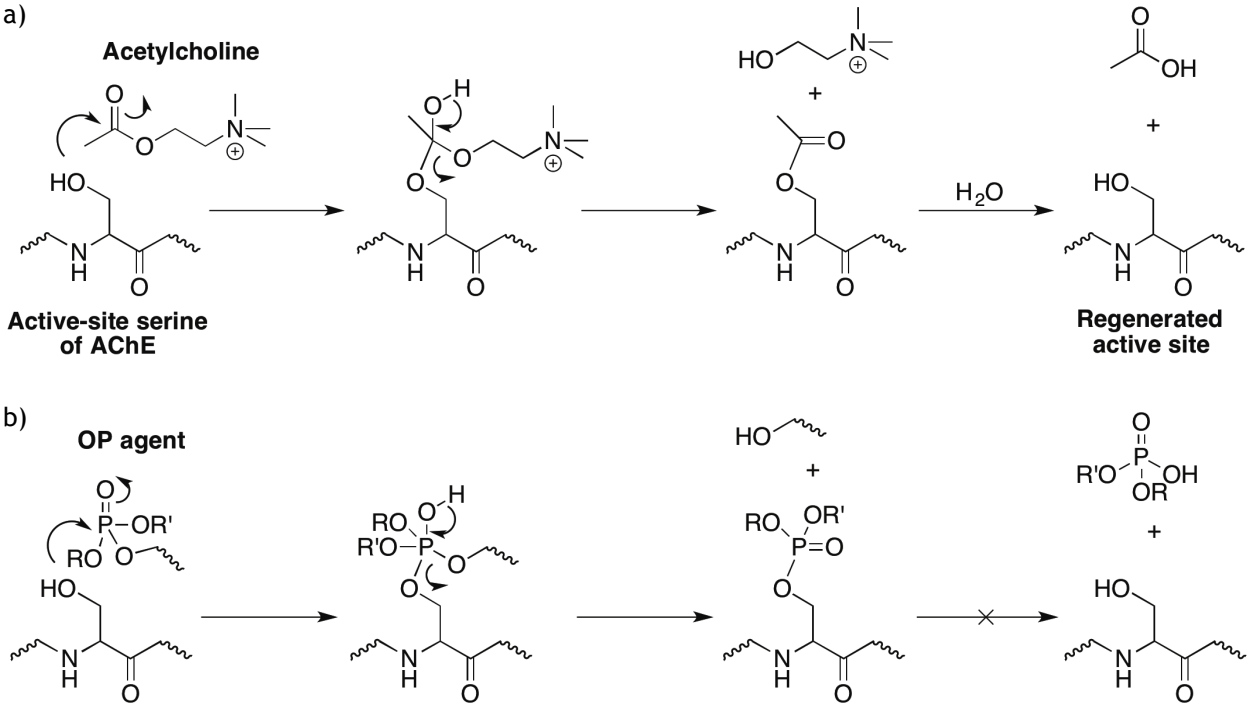

Scheme 5-1: Reaction mechanism of AChE in the presence of (a) ACh and (b) OP.

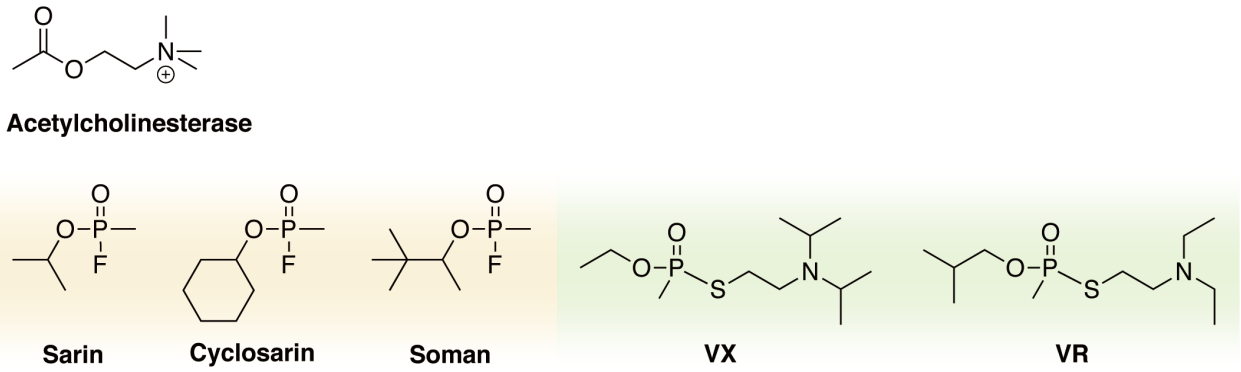

Scheme 5-2: Structures of acetylcholinesterase and common G-type (sarin, cyclosarin, soman) and V-type (VX, VR) organophosphate agents.

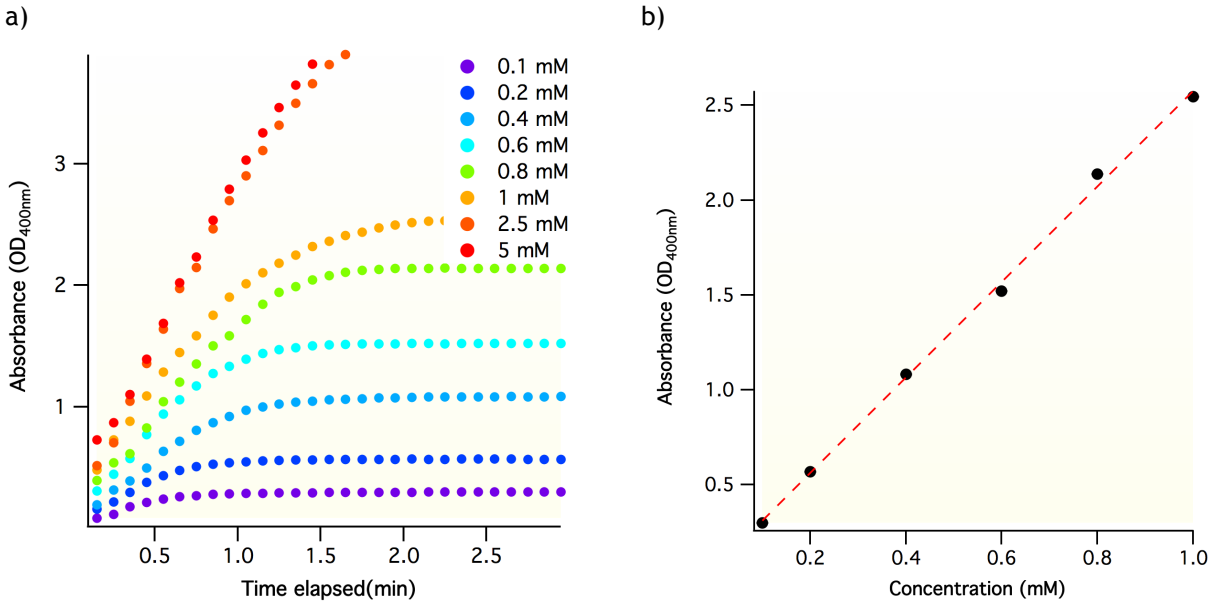

Figure 5-1: (a) Kinetic traces of *p*-nitrophenol formation at various concentrations of the starting reagent paraoxon and (b) extinction coefficient determination via Beer's Law for the hydrolysis product *p*-nitrophenol. The error bars represent standard deviation among 3 replicate readings.

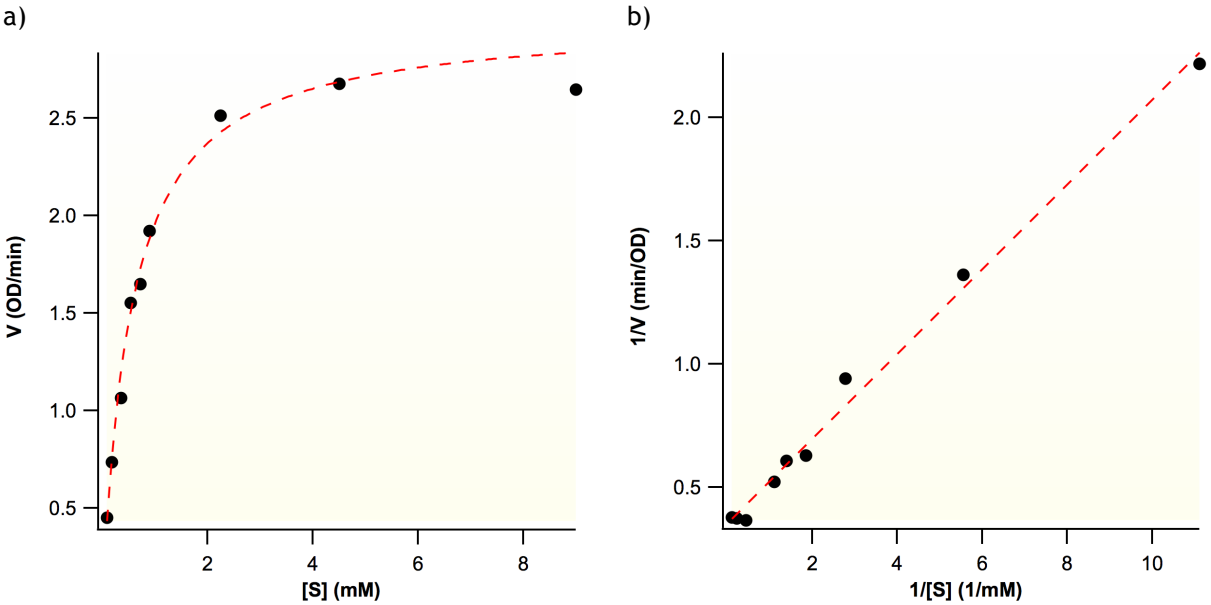

Figure 5-2: Kinetic parameters estimated using (a) the Michaelis-Menten or (b) the Lineweaver-Burk equation.

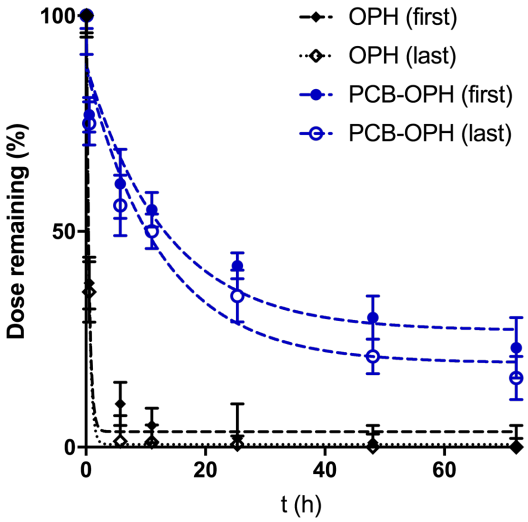

Figure 5-3: Circulation profiles of native and PCB-conjugated OPH after the first and final injections. The error bars represent standard deviation among three animals.

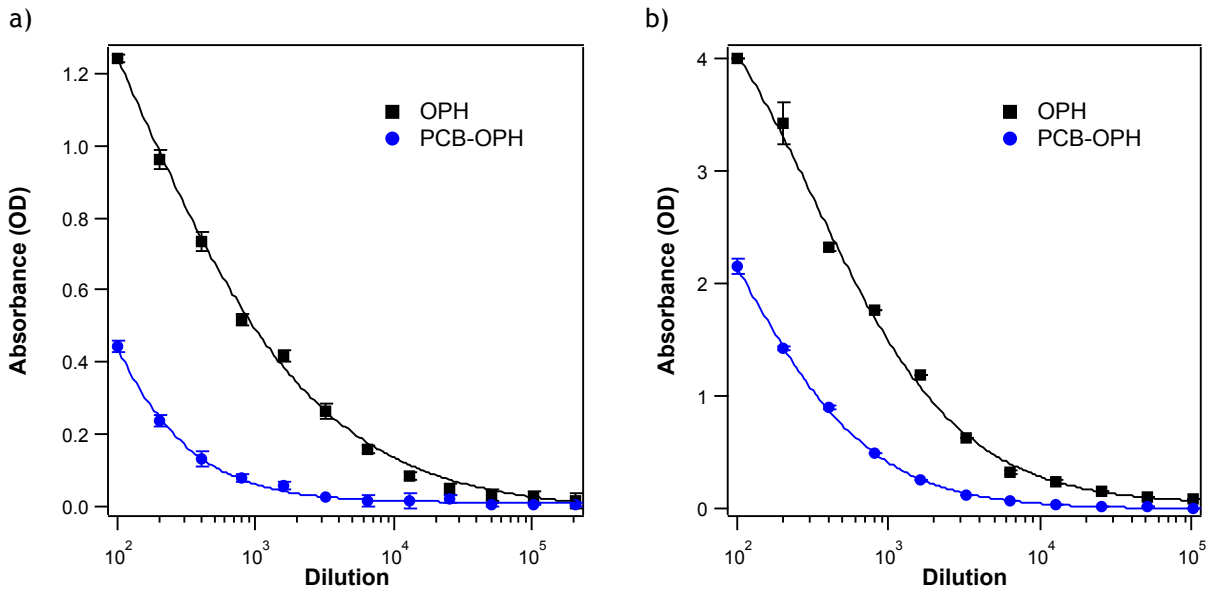

Figure 5-4: Antibody dilution profile of (a) IgM and (b) IgG elicited against OPH. PCB-OPH improved the IgM titer by 32-fold and the IgG titer by 16-fold. The error bars represent standard deviation.

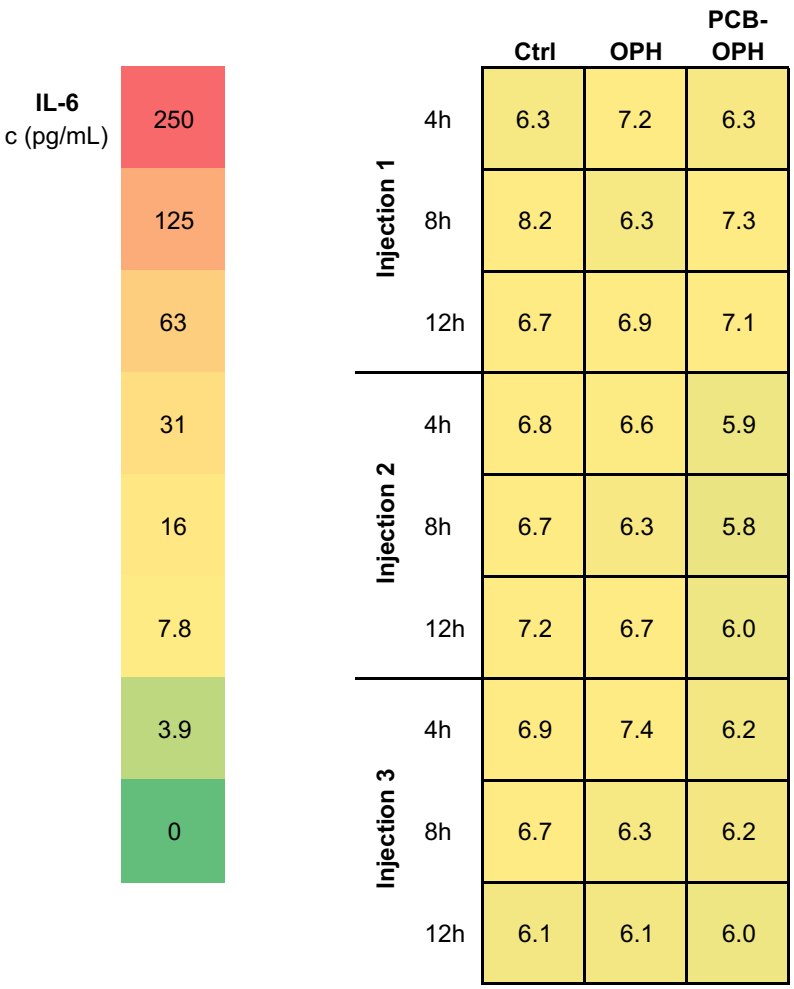

		Ctrl	OPH	PCB-OPH
Injection 1	4h	6.3	7.2	6.3
	8h	8.2	6.3	7.3
	12h	6.7	6.9	7.1
Injection 2	4h	6.8	6.6	5.9
	8h	6.7	6.3	5.8
	12h	7.2	6.7	6.0
Injection 3	4h	6.9	7.4	6.2
	8h	6.7	6.3	6.2
	12h	6.1	6.1	6.0

Figure 5-5: IL-6 cytokine quantification

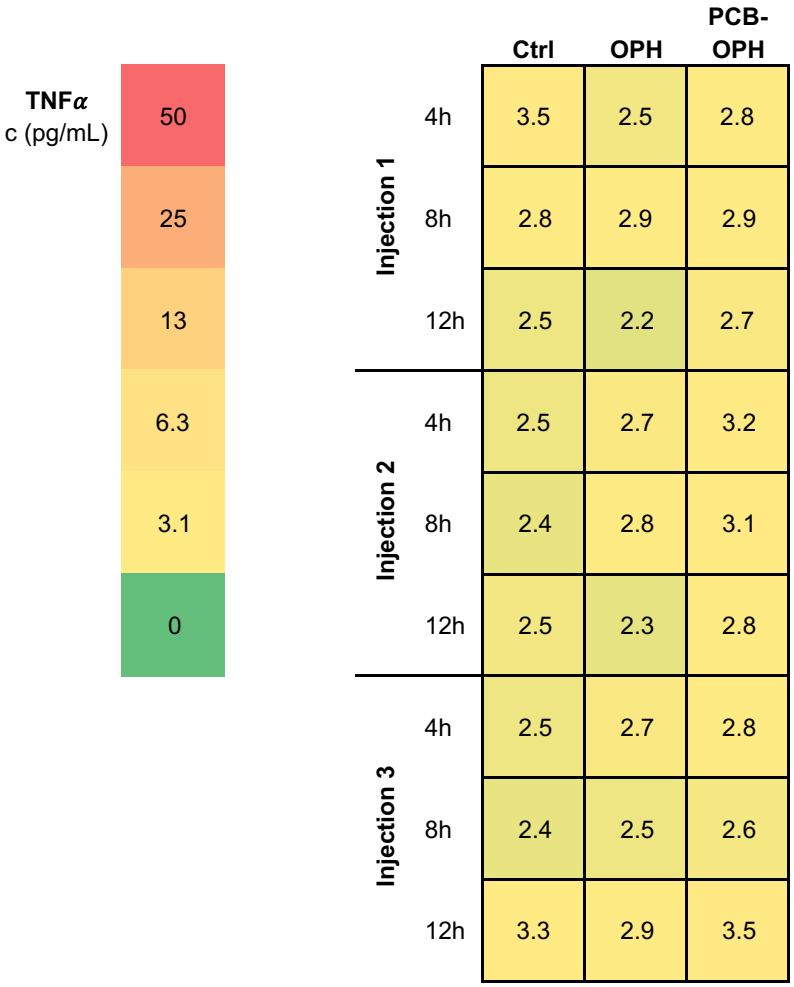

		Ctrl	OPH	PCB-OPH
Injection 1	4h	3.5	2.5	2.8
	8h	2.8	2.9	2.9
	12h	2.5	2.2	2.7
Injection 2	4h	2.5	2.7	3.2
	8h	2.4	2.8	3.1
	12h	2.5	2.3	2.8
Injection 3	4h	2.5	2.7	2.8
	8h	2.4	2.5	2.6
	12h	3.3	2.9	3.5

Figure 5-6: TNFα cytokine quantification.

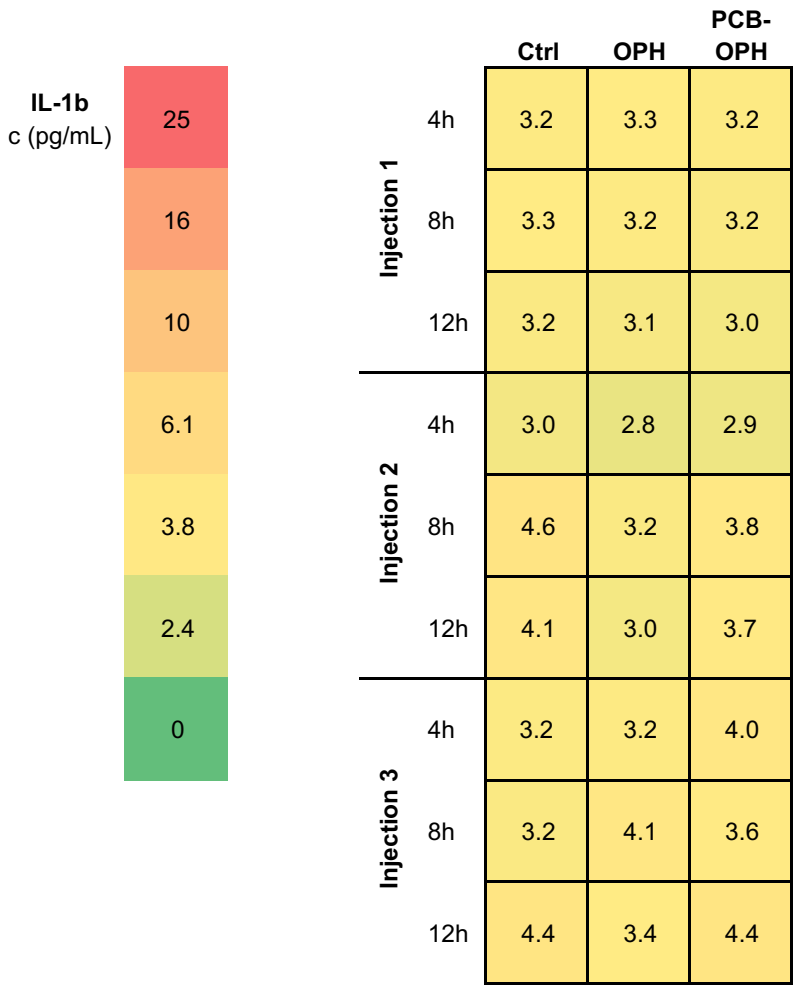

Figure 5-7: IL-1b cytokine quantification.

Table 5-1: Kinetic parameters of native OPH in 0.1 M sodium phosphate buffer supplemented with 0.1 mM $CoCl_2$ (pH 7.4) at 25 °C.

Fit Model	K_M (mM)	k_{cat} (1/s)	k_{cat}/K_M ($M^{-1}\cdot s^{-1}$)
Michaelis-Menten	0.35	14,000	4.0×10^7
Lineweaver-Burk	0.49	16,000	3.3×10^7

Table 5-2: Pharmacokinetic parameters of OPH and PCB-OPH conjugate.

Formulations	Half-life (h)	Relative bioavailability
OPH, first injection	0.5 (1x)	1x
OPH, last injection	0.3 (0.6x)	1x
PCB-OPH, first injection	9.2 (18x)	30x
PCB-OPH, last injection	8.7 (17x)	29x

5.7 References

1 Raushel, F. M. Bacterial detoxification of organophosphate nerve agents. *Current Opinion in Microbiology* **5**, 288-295, doi:10.1016/s1369-5274(02)00314-4 (2002).

2 Colovic, M. B., Krstic, D. Z., Lazarevic-Pasti, T. D., Bondzic, A. M. & Vasic, V. M. Acetylcholinesterase Inhibitors: Pharmacology and Toxicology. *Current Neuropharmacology* **11**, 315-335 (2013).

3 Russell, A. J., Berberich, J. A., Drevon, G. E. & Koepsel, R. R. Biomaterials for mediation of chemical and biological warfare agents. *Annual Review of Biomedical Engineering* **5**, 1-27, doi:10.1146/annurev.bioeng.5.121202.125602 (2003).

4 Saxena, A., Sun, W., Luo, C. Y. & Doctor, B. P. Human serum butyrylcholinesterase: In vitro and in vivo stability, pharmacokinetics, and safety in mice. *Chemico-Biological Interactions* **157**, 199-203, doi:10.1016/j.cbi.2005.10.028 (2005).

5 Chatonnet, A. & Lockridge, O. Comparison of butyrylcholinesterase and acetylcholinesterase. *Biochemical Journal* **260**, 625-634 (1989).

6 Ashani, Y. & Pistinner, S. Estimation of the upper limit of human butyrylcholinesterase dose required for protection against organophosphates toxicity: A mathematically based toxicokinetic model. *Toxicological Sciences* **77**, 358-367, doi:10.1093/toxsci/kfh012 (2004).

7 Saxena, A., Tipparaju, P., Luo, C. & Doctor, B. P. Pilot-scale production of human serum butyrylcholinesterase suitable for use as a bioscavenger against nerve agent toxicity. *Process Biochemistry* **45**, 1313-1318, doi:10.1016/j.procbio.2010.04.021 (2010).

8 Medical Identification and Treatment Systems (MITS): Bioscavenger. (United States Department of Defense, 2014).

9 Bigley, A. N., Xu, C. F., Henderson, T. J., Harvey, S. P. & Raushel, F. M. Enzymatic Neutralization of the Chemical Warfare Agent VX: Evolution of Phosphotriesterase for Phosphorothiolate Hydrolysis. *Journal of the American Chemical Society* **135**, 10426-10432, doi:10.1021/ja402832z (2013).

10 Leikin, J. B., Thomas, R. G., Walter, F. G., Klein, R. & Meislin, H. W. A review of nerve agent exposure for the critical care physician. *Critical Care Medicine* **30**, 2346-2354, doi:10.1097/00003246-200210000-00026 (2002).

11 Zhang, P., Sun, F., Tsao, C., Liu, S., Jain, P. *et al*. Zwitterionic gel encapsulation promotes protein stability, enhances pharmacokinetics, and reduces immunogenicity. *Proceedings of the National Academy of Sciences* **112**, 12046-12051, doi:10.1073/pnas.1512465112 (2015).

12 Yang, W., Liu, S., Bai, T., Keefe, A. J., Zhang, L. *et al*. Poly(carboxybetaine) nanomaterials enable long circulation and prevent polymer-specific antibody production. *Nano Today* **9**, 10-16, doi:10.1016/j.nantod.2014.02.004 (2014).

13 Zhang, L., Cao, Z. Q., Li, Y. T., Ella-Menye, J. R., Bai, T. *et al*. Softer Zwitterionic Nanogels for Longer Circulation and Lower Splenic Accumulation. *Acs Nano* **6**, 6681-6686, doi:10.1021/nn301159a (2012).

14 Keefe, A. J. & Jiang, S. Poly(zwitterionic)protein conjugates offer increased stability without sacrificing binding affinity or bioactivity. *Nature Chemistry* **4**, 60-64, doi:10.1038/nchem.1213 (2012).

15 Novikov, B. N., Grimsley, J. K., Kern, R. J., Wild, J. R. & Wales, M. E. Improved pharmacokinetics and immunogenicity profile of organophosphorus hydrolase by chemical modification with polyethylene glycol. *Journal of Controlled Release* **146**, 318-325, doi:10.1016/j.jconrel.2010.06.003 (2010).

CHAPTER 6

SUMMARY OF SIGNIFICANT FINDINGS AND FUTURE DIRECTIONS

6.1 Notable results

6.1.1 Undetectable polymer-specific antibody response

We developed zwitterionic polymers with the intent of eliciting as few immune responses. Under our current validated detection systems, we could not observe polymer-specific antibody generation in the isotypes examined, IgM and IgG. We have conjugated these polymers to a few different immunogenic proteins, which should function as large carriers that may initiate antibody responses when introduced repeatedly in the same animal. However, we found antibodies generated against another polymer, poly(ethylene glycol) (PEG), but not poly(carboxybetaine) (PCB). We hypothesize this is largely due to two characteristics: (1) PCB is a polymer of an analogue of a naturally occurring amino acid, which suggests the structure might be tolerated by the immune system during early development, and (2) PCB is super hydrophilic, unlike the amphiphilic PEG, and hydrophobicity has been demonstrated to correlate with immunogenicity[1,2].

6.1.2 Superior protection of immunogenic therapeutic proteins

In parallel with the polymer-specific antibody responses, we also studied the decrease in protein-specific reactions. As therapeutic proteins are often expressed in bacterial systems, they are likely to be targets of the immune system and removed upon recognition. We investigated the effect of several different polymer lengths and grafting densities, with the goal of determining an ideal combination for maximum protein protection. Our results demonstrated that for the protein systems studied, the PCB polymer with hydrodynamic-size equivalent to 10-kDa PEG is the optimal size. Its conjugation caused in 81x decrease in IgM and 243x in IgG[3] compared to the PEGylated enzyme of the same polymer density. We have also demonstrated a lack of circulating cytokines that are markers of acute inflammatory responses. These are encouraging results in our development of an alternative polymer conjugation strategy to the industry standard PEG.

6.2 Future endeavors

Antibody responses are just one branch of the immune system, whose activation is complex and interrelated. In order to gather a more complete picture towards practical application of our polymer conjugation system, we must study other branches of the immune system. For example, pre-clinical studies would entail assessment of immune cell activation, which can be monitored by isolating immune cells of the peripheral blood, spleen, thymus, and lymph nodes after sample administration. The cytokines produced in vitro in response to the addition of polymer-protein conjugates would elucidate which immune pathways are activated. We also need to investigate the maximal tolerated dose (single and multiple) of polymer conjugates, which can be observed in physical changes (e.g. weight loss, blood protein content, tissue morphology) due to increasing higher amount of conjugates injected. The results from these preliminary studies would then suggest further studies pertinent to deciphering the suitability of PCB as a therapeutic.

6.3 References

1 Sherman, M. R., Williams, L. D., Sobczyk, M. A., Michaels, S. J. & Saifer, M. G. P. Role of the Methoxy Group in Immune Responses to mPEG-Protein Conjugates. *Bioconjugate Chemistry* **23**, 485-499, doi:10.1021/bc200551b (2012).

2 Saifer, M. G. P., Williams, L. D., Sobczyk, M. A., Michaels, S. J. & Sherman, M. R. Selectivity of binding of PEGs and PEG-like oligomers to anti-PEG antibodies induced by methoxyPEG-proteins. *Molecular Immunology* **57**, 236-246, doi:10.1016/j.molimm.2013.07.014 (2014).

3 Liu, S. & Jiang, S. Zwitterionic polymer-protein conjugates reduce polymer-specific antibody response. *Nano Today* **11**, 285-291 (2016).